Deep Learning Based Abnormal Gait Classification System Study with Heterogeneous Sensor Network

UNIVERSITY OF TURKU
Department of Future Technologies
Master of Science in Technology Thesis
Networked Systems Security
September 2019
Shubao Yin

Supervisors:
Wei Chen
Syed Rameez Kakakhel

UNIVERSITY OF TURKU
Department of Future Technologies

SHUBAO YIN: Deep Learning Based Abnormal Gait Classification System Study with Heterogeneous Sensor Network

Master of Science in Technology Thesis, 83 p., 0 app. p.
Software Engineering, Embedded Electronics, and Communication Technology
September 2019

Gait is one of the important biological characteristics of the human body. Abnormal gait is mostly related to the lesion site and has been demonstrated to play a guiding role in clinical research such as medical diagnosis and disease prevention. In order to promote the research of automatic gait pattern recognition, this paper introduces the research status of abnormal gait recognition and systems analysis of the common gait recognition technologies. Based on this, two gait information extraction methods, sensor-based and vision-based, are studied, including wearable system design and deep neural network-based algorithm design.

In the sensor-based study, we proposed a lower limb data acquisition system. The experiment was designed to collect acceleration signals and sEMG signals under normal and pathological gaits. Specifically, wearable hardware-based on MSP430 and upper computer software based on Labview is designed. The hardware system consists of EMG foot ring, high-precision IMU and pressure-sensitive intelligent insole.

Data of 15 healthy persons and 15 hemiplegic patients during walking were collected. The classification of gait was carried out based on sEMG and the average accuracy rate can reach 92.8% for CNN. For IMU signals five kinds of abnormal gait are trained based on three models: BPNN, LSTM, and CNN. The experimental results show that the system combined with the neural network can classify different pathological gaits well, and the average accuracy rate of the six-classifications task can reach 93%.

In vision-based research, by using human keypoint detection technology, we obtain the precise location of the key points through the fusion of thermal mapping and offset, thus extracts the space-time information of the key points. However, the results show that even the state-of-the-art is not good enough for replacing IMU in gait analysis and classification. The good news is the rhythm wave can be observed within 2 m, which proves that the temporal and spatial information of the key points extracted is highly correlated with the acceleration information collected by IMU, which paved the way for the visual-based abnormal gait classification algorithm.

Keywords: deep neural network, abnormal gait analysis, IMU, sEMG

图尔库大学
未来科技系
殷书宝: 基于深度学习与异构传感网络的异常步态分类系统研究
硕士论文，共 83 页，0 附录，
涉及软件工程，嵌入式电子和通信技术，
写于 2019 年九月

步态指人走路时表现出来的姿态，是人体重要生物特征之一。异常步态多与病变部位有关，作为反映人体健康状况和行为能力的重要特征，其被论证在医疗诊断、疾病预防等临床研究中具有指导作用。为了促进步态模式自动识别的研究，本文介绍了异常步态识别的研究现状，系统地分析了常见步态识别技术以及算法,以此为基础研究了基于传感器与基于视觉两种步态信息提取方法,内容包括可穿戴系统设计与基于深度神经网络的算法设计。

在基于传感器的研究中,本工作开发了下肢步态信息采集系统,并利用该信息采集系统设计实验,采集正常与不同病理步态下的加速度信号与肌电信号,搭建深度神经网络完成分类任务。具体的,在系统搭建部分设计了基于 MSP430 的可穿戴硬件设备以及基于 Labview 的上位机软件，该硬件系统由肌电脚环，高精度 IMU 以及压感智能鞋垫组成，该上位机软件接收、解包蓝牙数据并计算出步频步长等常用步态参数。

在基于运动信号与基于表面肌电的研究中，采集了 15 名健康人与 15 名偏瘫病人的步态数据，并针对表面肌电信号训练卷积神经网络进行帕金森步态的识别与分类，平均准确率可达 92.8%。针对运动信号训练了反向传播神经网络，LSTM 以及卷积神经网络三种模型进行五种异常步态的分类任务。实验结果表明，本工作中步态信息采集系统结合神经网络模型，可以很好地对不同病理步态进行分类，六分类平均正确率可达 93%。

在基于视觉的研究中，本文利用人体关键点检测技术，首先检测出图片中的一个或多个人，接着对边界框做图像分割，接着采用全卷积 resnet 对每一个边界框中的人物的主要关节点做热力图并分析偏移量，最后通过热力图与偏移的融合得到关键点的精确定位。通过该算法提取了不同步态下姿态关键点时空信息，为基于视觉的步态分析系统提供了基础条件。但实验结果表明目前最高准确率的人体关键点检测算法不足以替代 IMU 实现步态分析与分类。但在 2m 之内可以观察到节律信息，证明了所提取的关键点时空信息与 IMU 采集的加速度信息呈现较高相关度，为基于视觉的异常步态分类算法铺平了道路。

关键词：深度神经网络，异常步态分析，IMU，表面肌电，人体关键点检测

Table of Contents

Abbreviations and Acronyms

IMU	Inertial Measurement Unit
DMP	Digital Motion Processor
sEMG	Surface Electromyogram
BLE	Bluetooth Low Energy
SoC	System on Chip
MCU	Micro Controller Unit
DCO	Digitally Controlled Oscillator
RISC	Reduced Instruction Set Computer
SPI	Serial Peripheral Interface
I2C	Inter-Integrated Circuit
ADC	Analog-to-Digital Converter
GPIO	General Purpose Input Output
UART	Universal Asynchronous Receiver/Transmitter
PCB	Printed Circuit Board
FPC	Flexible Printed Circuit
ROM	Read-only Memory
ANN	Artificial Neural Network
CCD	Charge Coupled Device
FSRS	Force Sensing Resistors
PCA	Principal Component Analysis
SMOTE	Synthetic Minority Oversampling Technique
SPCA	Supervised Principal Component Analysis
GEI	Gait Energy Image
FOG	Freezing of Gait

HMM	Hidden Markov Model
ROC	Receiver Operating Characteristic
AUC	Area Under Curve
EER	Equal Error Rate
SDK	Software Development Kit
GRF	Ground Reaction Force
DWT	Discrete Wavelet Transform
NNC	Nearest Neighbor Classifier
CNN	Convolutional Neural Network
BPNN	Back Propagation Neural Network
RNN	Recurrent Neural Network
LSTM	Long Short Term Memory
RAM	Random Access Memory
USB	Universal Serial Bus
PG	Parkinson's Gait

1 Introduction

Gait, as the manner of walking, is an idiosyncratic and perceptible biological behavioral feature of a person. Normal gait has the following characteristics, including stability, periodicity, rhythm, and individual differences. Generally, gait can be classified into normal gait and pathological gait. The pathological gaits may mainly cause due to hemiplegia, Parkinson's disease, myopathy, and pain. It includes typically gaits, namely, hemiplegic gait, Parkinson gait, gluteus medius gait, steppage gait and so on[1]. By classifying the walking pattern of people, gait recognition can be used to detect people's identities. Gait also has many other applications in fields like medical treatment and abnormal behavior detection.

Musculoskeletal diseases are one of the main causes of abnormal gait, which have a significant impact on society, it may cause long-term disability. With the aging of the population in some countries, these problems will increase rapidly in the future[2]. In the field of medicine, researchers have studied gait as a unique feature of human beings[3]. Medical studies have shown that gait analysis can diagnose abnormal gait and pathological gait such as hemiplegia[4], [5]. Etiological analysis of human athletic system and nervous system diseases can provide a lot of important information for the reconstruction, prevention, and rehabilitation of walking ability of patients who are suffering from paralysis or other diseases. Compared with other biological characteristics, gait has the characteristics of long-distance, inviolability, difficult to hide and camouflage, and easy to collect. Such characteristics show great potentials in computer vision-based gait study. The relative position of the key points of human skeleton and the angle of joints are different. Therefore, we can use the key points of the human skeleton to describe the gait characteristics and apply them to the recognition and prediction of human motion[6].

Identification of normal and pathological gaits could provide deep insights to

understand various human movement patterns across different gait pathologies. However, traditional gait assessment is mainly based on clinical observations. It is a subjective and time-consuming decision-making process for clinicians. To address these issues, automatic methods to discriminate between normal and pathological gaits have been attracted widespread attention.

Gait analysis[3] is a kind of biomechanical research method, which uses the concept and processing method of sports biomechanics to analyze human walking. Gait analysis is the acquisition of human motion information, such as ground reaction force, force path, gait stability, stride frequency and so on, without disturbing human natural activities. It can be applied to the following aspects:

(1) To assess abnormal gait.

(2) To assess the degree and nature of abnormal gait.

(3) To provide necessary data for the analysis of the causes of abnormal gait and how to correct abnormal gait, thus formulate a treatment plan.

(4) To evaluate the effect of rehabilitation treatment.

By identifying the abnormal gait, we can find out whether the person under guardianship has an abnormal condition, so as to take timely measures.

The remaining chapters are assigned as follows. We present technological background and related works in chapter 2 as well as a brief introduction to this work. In chapter 3, the structure of the experiment platform and the proposed system are introduced in detail. The design of the neural-network-based algorithm for pathological gait analysis is proposed in chapter 4 and 5, including the design of experiments and the discussion of results. The conclusion of the work is summarized in chapter 6.

2 Background & Related Works

2.1 Human Motion Recognition and Gait Analysis

Basically, research on abnormal gait recognition consists of two types, sensor based[7], [8] [9]and video based[10]. For sensor-based studies, they mainly contain two aspects, which are the study, design, build and development of hardware platform, and the improvement of exiting gait recognition algorithm[11], [12].

For video-based studies, from feature extraction to feature fusion, and design of classifying machines, many relevant pieces of research have been done internationally. Ziba Gandomkar et al.[13] proposed a markless vision-based technique for extracting a set of features from the human walking sequence for differentiating normal and abnormal gait. The classification steps are as follows: firstly, the contour and its boundary box are extracted in each frame. Then, the contour is normalized according to the height of the contour. Finally, the gait Fritz pattern is adopted for feature extraction. Murase, H, and Sakai, R[14] describe a new method to calculate the spatial-temporal correlation of the feature space representation of the parameter effectively in moving target recognition. Parametric feature space compactly represents the time variation of image sequence through the tracks in feature space. This representation reduces the computational cost of correlation-based comparison between image sequences. In Élodie Desseré and Louis Legrand's [15] study, a complete method of gait analysis using an unmarked system is proposed. The designed acquisition system consists of three CCD cameras calibrated synchronously. The legs of walkers are recognized in a gray image sequence, reconstructed in three-dimensional space, and the movement of the human body in gait activity is analyzed. This paper introduces a three-dimensional model of the human joint based on conic super conic. The image sequence is segmented based on a motion by a morphological operator, and the boundary of the moving leg is extracted. Next, the least square method (LMS) is used to reconstruct the human body

in order to determine the position of the human body in three-dimensional space. Finally, spatial coherence is applied to the reconstructed curve to better fit the anatomical structure of the leg and consider the joint model. Researchers also proposed a synthesis method to compose gait sequences to the canonical-viewed ones based on the planar homography, thus reduce the directional dependency[16], [17]. Based on the overall consideration of speed and effect, Han et al.[18] proposed a new spatiotemporal gait representation method, called gait energy image (GEI), which is proposed to represent the gait characteristics of human beings and realize the gait recognition of individuals. Based on this work, in Theekhanont et al.'s work [19] GEI was transformed into a trace transform image. The threshold value of the tracking transformed image is used to calculate the mode tracking transformed image to develop the mode tracking transformation. Finally, they use template matching for recognition.

The research of abnormal gait based on non-video sensors can be divided into two aspects: one is the research and establishment of a hardware platform for abnormal gait recognition for elderly monitoring, the other is the improvement and optimization of abnormal gait recognition algorithm (classifier).

Howell, Adam M., et al.[20] measured the ground support force by placing 12 pressure sensors on the insoles, and the gait was further analyzed. To determine the ground reaction force and the moments corresponding, subject-specific linear regression models were used. Which is corresponding to ankle dorsiflexion/plantarflexion, knee flexion/extension, and knee abduction/adduction? Other studies using force sensor includes[21], [22] use a hidden Markov model (HMM) to analyze the gait stage in gait movement. The ground contact force (GRF) obtained by intelligent shoes is used as the observation data in HMM, and the posterior probability in HMM is used to infer the gait stage.

In [23], [24], a gait analysis system based on a single accelerometer is described to

evaluate the dynamic gait characteristics. The acceleration data of normal people and Parkinson's disease patients were recorded continuously, from which the peak value of gait was extracted, and the relationship between gait period and vertical gait acceleration was evaluated. By fitting the model equation, the quantitative index of walking behavior was obtained. The mean index of patients with gait disorders was statistically lower than that of normal people. [25] presents a wearable device based on IMU and its associated stride detection algorithm to analyze gait information for patients with Alzheimer's disease (AD).

Abnormal gait recognition based on one kind of sensor (accelerometer or pressure sensor) is mainly introduced. The related research using multiple sensors is introduced below. For example:

C. Senanayake et al.[26] proposed a system to obtain ground contact force and knee joint angles. The system consists of four force-sensitive resistors and two inertial sensors. They also build the software application to be used in a clinical environment that is user-friendly and allows users to perform gait analysis without knowledge in the area.

A wireless wearable system was developed by Stacy J Morris Bamberg et al.[27] to provide gait analysis outside the motion laboratory. The sensor kit consists of three orthogonal accelerometers and gyroscopes as well as four force sensors. Two bidirectional bending sensors, two dynamic pressure sensors and an electric field height sensor were also used. "Gaithoe" can be designed to wear on any shoe without disturbing the gait, and can collect data in any environment for a long time without interference.

Some other studies deal with gait analysis using one camera. For example, a clinical measurement system based on the elliptical hierarchical tree structure is proposed in

[28]. However, the system is limited to the front parallel (side view) gait and does not provide a complete three-dimensional measurement.

2.2 Deep Learning and Human Skeleton Key Point Detection

Meng Chen et al.[29] presents a method using a hidden Markov model for modeling human abnormal gait. The system modeling normal gait, toe-in and toe-out gait abnormalities patterns. An IMU is employed to measure angular velocities and accelerations of the human foot. One bend sensor and four force-sensing resistors (FSRs) are arranged on the insole for force and flexion information acquisition. For feature generation, principal component analysis (PCA) is mainly used and multi-pattern modeling hidden Markov model (HMM) is used. The experiment results show the proposed models are robust and efficient.

Nguyen Trong-Nguyen et al.[2] proposed an approach for detecting abnormal gait. Their model is based on a human joint skeleton in time series instead of using the silhouette, color image or Spatio-temporal volume. They decompose the normal gait images sequence by gait cycles and each instant posture is represented by a feature vector. The vector describes relationships between pairs of the bone of the lower body. A clustering technique was used and those vectors are then converted into codewords. On Kinect skeleton and marker-based data, the experimental results show that the method does well in distinguishing normal and abnormal gaits, and the overall accuracy can reach 90.12%.

2.3 Analysis of Advantages and Disadvantages

Researchers have conducted researches on recognition of abnormal gait for a long time, and many techniques, systems, and algorithms have been demonstrated. For sensor-based research, IMU is the most popular one since it is intuitive and detailed.

While multi-sensor gait analysis contains gyroscopes, accelerometers, surface EMG, planta pressure and so on. With the help of these multi-source heterogeneous sensors, more data can be gathered during walking and much data fusion algorithms can be explored. On the other hand, video-based research on recognition of abnormal gait is not so much a problem in the field of biomedical engineering as a problem in the field of computer vision. To analysis the information of gait, the skeleton needs to be extracted, while the precision of the key-points model may not good enough for abnormal gait analysis.

To sum up, the sensor-based system has the advantages of cheap and precision, but it needs a system to wear or adorn, which is an inconvenience to users. It is also worth mentioning that traditional study usually forces on the methods of feature extraction or design of the system. The video-based study is easy to use but the accuracy still needs to be improved.

2.4 Study Target and System Solution

The purpose of this study is to explore the new gait recognition system and algorithm design. First, a heterogeneous sensor networks system was built as our experiment platform. Two wearable motion sensors were used to acquire the motion signals. Second, ANNs (BPNN, LSTM, and CNN) based pathological gait classifiers were used to identify different pathological gaits. At last, the key points of the human skeleton have extracted and analyzed the ability to replacing low-precision wearable devices.

3. System & Platform Design

In this part, we launch the design procedure from the requirement design and the architecture of the top-level system is presented. Then the hardware selection and design decision-making will be introduced and discussed. Finally, the hardware structure of the system is given and the basic functional unit testing, as well as joint testing, was demonstrated. Experiments were carried out to investigate the system performance, which demonstrated the potential of the proposed system in home-based scenarios and clinical practice.

3.1 Top-level System Architecture

In this work, a novel wearable multimode system for lower limb activity evaluation and gait recognition comprised of a multi-functional band, plantar pressure distribution sensor and a local terminal connected to an upper machine platform is presented. This proposed system can acquire the necessary data for lower limb activity evaluation and gait recognition based on clinical practice. By using the proposed system, we can gather necessary data for ANN (artificial neural network) based gait classification research, and the therapists can distribute the specific training plans based on the evaluation results through the system for the patients to rehabilitate more efficiently.

Inertial Measurement Units (IMU) and physiological signal front end with carbonized foam electrode are embedded in the proposed system to obtain motion signals and electromyogram (EMG) signals.[30] Furthermore, a novel plantar pressure distribution sensor using flexible pressure sensors, flexible conductive lines, and fabric materials is proposed to get the plantar pressure distribution. The carbonized foam electrode and proposed plantar pressure distribution sensor enable a more convenient evaluation and rehabilitation process. Patients can switch between two different wearing modes with

EMG signals on and off.

Figure 3.1 shows the top-level architecture of the hardware part, whose goal is to gather information about the physiological signals we needed. We designed three types of physiological signals acquisition unit, and all of them were connected to the MCU (Micro Controller Unit) through SPI (Serial Peripheral Interface) or I2C (Inter-Integrated Circuit) or ADC (Analog-to-Digital Converter). The data, after processed by the MCU, submitted to the upper machine through UART (Universal Asynchronous Receiver/Transmitter).

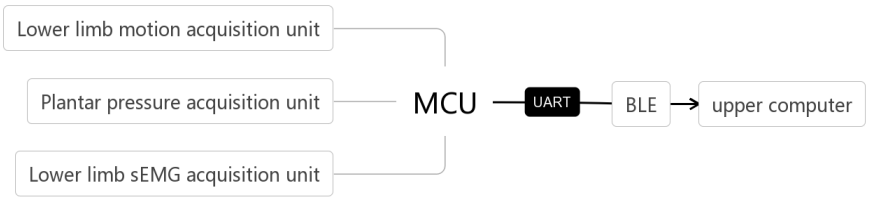

Figure 3.1 Top-level system architecture of gait information acquisition system

3.2 requirements for the system

The remote rehabilitation system in this project needs highly interdisciplinary research, involving many different fields such as demand research, medical science, sensing technology, hardware design, software design, human interaction, etc. Therefore, before designing the system scheme, we had a group discussion and research with doctors, designers, and summarized the list of requirements for the system.

We launched the design procedure from the requirement design based on the need-finding with rehabilitation patients and medical therapists. Based on the need-finding results, we proposed the following requirements:

- Precise, continuous and multidimensional data collecting on the lower limbs with limited disturbance to subjects

- Data management for further use, like retrospective analysis and longitudinal study.
- Some reserve ports for further expanding modules.

Table3.1 List of requirements for remote rehabilitation system of lower extremities

Lower extremity data comprehensive acquisition system	
Function	Motion Inertia Signal Collection
	sEMG Signal Collection
	Signal collection of plantar pressure distribution
	Wireless transmission
Easy-using	Non-Intrusive
	Rechargeable
	Comfort
	Disassembling
	The high degree of permanence to wear and washing
	Safety of data transfer and use
	Easy to produce and reproduce
	Stable sensor
The upper machine	
Function	Data storage
	Data presentation
	Data interaction and fusion
	Action and Data Visualization
	Data Security and Data Encryption
Easy-using	Easy to operate
	Easy to understand

3.3 hardware design decisions

Based on the requirement list, we design the system framework. The system is roughly divided into three parts: data acquisition, data processing, and system software.

For data acquisition, three kinds of sensors are needed. They are a sensor for motion inertia signal collection, sEMG signal collection, and plantar pressure distribution collection.

MPU9250 integrates 3-axis gyroscope, 3-axis accelerometer, and 3-axis magnetometer, and the output is 16-bit digital. The data can be exchanged through the integrated circuit bus (IIC) interface to the microcontroller, and the transmission rate can reach 400 kHz/s. The angular velocity measurement range of the gyroscope is up to 2000 (degrees /s), and it has good dynamic response characteristics. The maximum measurement range of accelerometer is ±16g, g is gravitational acceleration, and the static measurement accuracy is high enough. Its magnetometer uses a high-sensitivity Hall-type sensor for data acquisition and the measurement range of magnetic induction intensity is 4800 UT, which can be used for auxiliary measurement of yaw angle. Fig 3.2 shows the chip's internal block diagram.

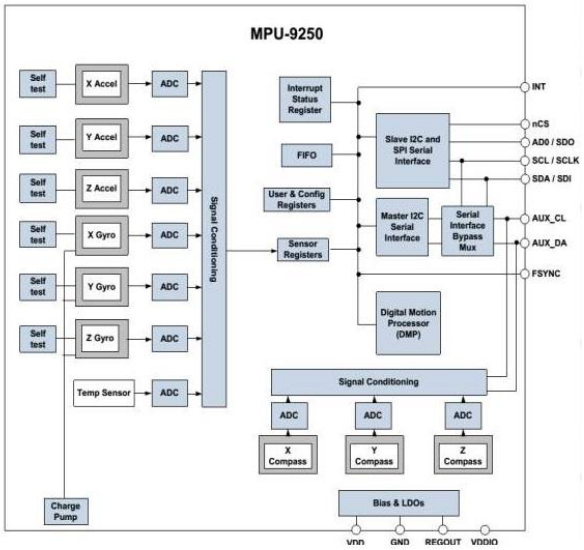

Fig 3.2 Internal block diagram of MPU9250

Besides, The hardware acceleration engine of MPU9250, named Digital Motion Processor (DMP) can integrate nine-axis sensor data and output complete nine-axis fusion calculus data to the application. With DMP, we can use the MPL (Motion Process Library) provided by the InvenSense company, which is very convenient to realize attitude calculation, reduces a load of motion processing operation on the operating system, and greatly reduces the difficulty of development. Based on this discussion, we choose MPU9250 as the sensor for motion inertia signal collection.

AD8232 is an integrated front-end, which is suitable for signal conditioning and monitoring of bioelectric signals. AD8232 can amplify electrophysiological signals such as EMG and ECG, and suppress electrode half-cell potential. It has a smaller size and low power consumption. It can amplify bioelectrical signals as analog output. Because the bioelectric signal is very small and easy to be disturbed by the outside world, the AD8232 bioelectric monitor can help to obtain the obvious bioelectric signal after amplification through the amplifier. The typical output analog value of EMG signal after amplification is 1~2V order of magnitude, which facilitates the

analog-to-digital conversion of the latter stage. The typical structure of double-lead is shown in Fig 3.3 below.

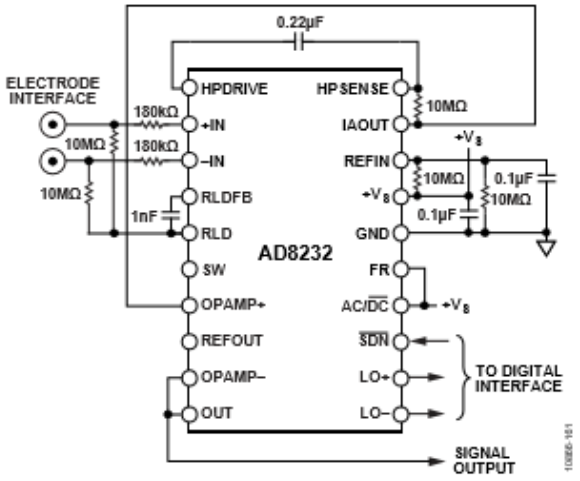

Fig 3.3 A typical double lead circuit of AD8232

Therefore, EMG signals collected by flexible carbonized sponge electrodes are filtered by AD8232 combined with peripherals. Based on this discussion, we choose AD8232 as a sensor for sEMG Signal collection.

The signal transmission module chip of this system adopts the FSC-BT822 Bluetooth module. The device has good compatibility and is easy to connect with computers, mobile phones, tablets, and other devices. The serial port of the Bluetooth module is connected with the serial port of MSP430F5529. Complies with Bluetooth 4.2 dual mode protocols (BR/EDR/BLE), FSC-BT822 is a fully integrated Bluetooth module. It supports SPP, HID, GATT, Beacon, profiles. It integrates the Baseband controller and MCU in a small package(Integrated chip antenna), so the designers can have better flexibilities for the product shapes. Fig 3.4 shows the BLE module we used.

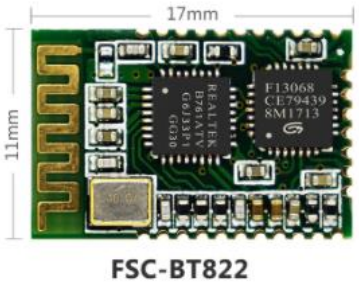

Fig 3.4 FSC-BT822

After selection among various pressure material, our system adopts Velostat pressure material from 3M company, this conductive material (also known as "Veloster" or "linqstat") is a good addition to the wearable/sensor hack kit. It is pressure-sensitive: squeezing it will reduce the resistance, so it is very convenient to make flexible sensors. It's much cheaper than off the shelf pressure or bend sensors, which is lower cost and better flexibility. The physical properties are opaque black with a thickness of about 100 um. Its electrical property is piezoresistive, that is, resistance decreases with the increase of pressure. This material was originally used for ESD (Electro-Static Discharge) bags, but at present, some researchers have used this material as a simple pressure sensing system. Based on these discussions, the plantar pressure array acquisition module is made of Velostat material and flexible plastic film conductive tape. Fig 3.5 shows this material named Velostat.

Fig 3.5 the Velostat conductive material

MSP430F5529 MCU is chosen as the main processing module of the system. TI MSP430 series ultra-low-power microcontrollers are composed of a number of devices with peripheral devices for various applications. This architecture, combined with a wide range of low power consumption modes, can be optimized to extend battery life in portable measurement applications. What's more, the microcontroller has a powerful 16 bit RISC CPU, 16-bit register and constant generator, which helps to improve code efficiency. The digital control oscillator (DCO) allows the device to wake up from a low power mode to an active mode in 3.5 mesh.

Msp430f5529 microcontroller integrates USB and PHY supporting DMA, four 16 bit timers, USB 2.0, two USCIS, a hardware multiplier, an RTC module with alarm function, a high-performance 12-bit analog-to-digital converter (ADC) and 63 I / O pins. Its typical applications include analog and digital sensor systems, data recorders and other applications that need to be connected to various USB hosts.

To sum up, MSP430 series MCU is a 16-bit mixed-signal processor with ultra-low power consumption and Reduced Instruction Set Computer (RISC). Compared with other microcontrollers, this series of microcontrollers have the advantages of ultra-low power consumption and abundant peripherals on-chip, which are very suitable for EMG signal processing. MSP430F5529 is selected as the control chip in this system. In MSP430 series chips, MSP430F5529 can not only meet the functional requirements but also has lower power consumption and cost overall. Figure 3.6 shows the structure of the MSP430F5529.

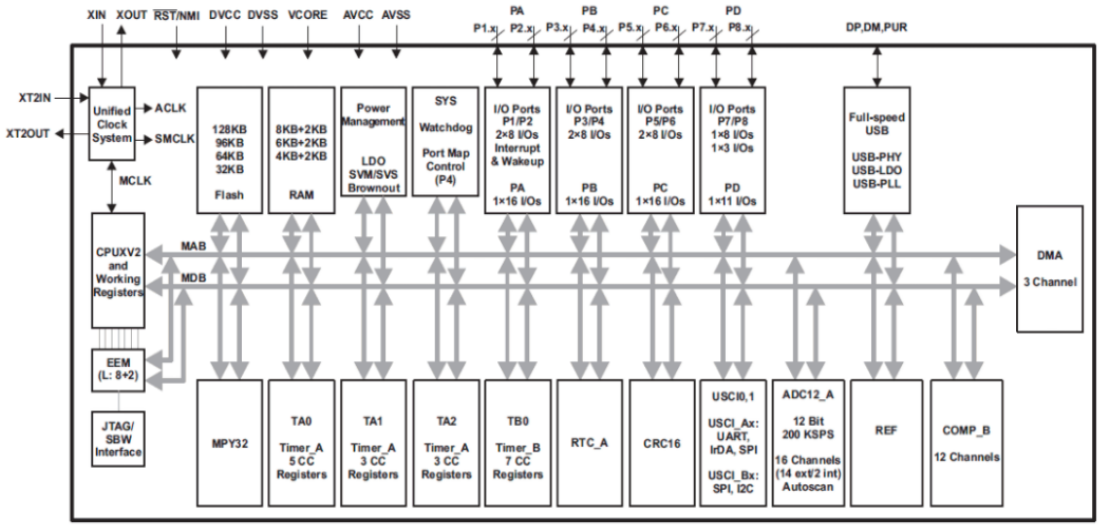

Fig 3.6 The structure of MSP430F5529

We begin to design three types of physiological signals acquisition units based on these decisions. And all of them were connected to the MCU (Micro Controller Unit) through SPI (Serial Peripheral Interface) or I2C (Inter-Integrated Circuit) or ADC (Analog-to-Digital Converter).

3.4 System Implementation

From clinical practice, there are various parameters for lower limb activity evaluation and rehabilitation status. There are three key points among them, which are the myodynamia, balance ability and lower limb range of motion (ROM). To make our system and clinical practice seamless, our proposed system should acquire these three parameters for evaluation.

Based on the system architecture and clinical requirements, we design the data flow of our system. The completed data flow of the proposed system contains four parts, data collection, signal pre-processing, data transmission and data analysis and display. The

data flow sketch is shown in Fig 3.7. The wearable multimode system collects plantar pressure distribution, motion signals, and EMG signals. Then the microcontroller unit (MCU) fixed in the multifunctional band will process the signals and transmit them to the local mobile terminal via Bluetooth. Finally, the mobile terminal together with the cloud platform will analyze and store the data.

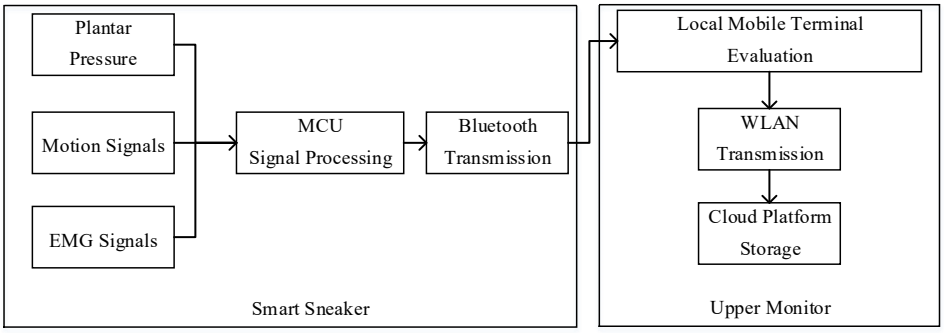

Fig 3.7 Data flow sketch

In this section, the technical details about the whole system are presented. The overall wearable multimode system consists of two parts, a multifunctional band with a plantar pressure sensor as well as a mobile terminal with the application. For detail, the signal acquisition module includes an EMG module, two IMU modules, and a planter pressure acquisition module. As for the data acquisition, a new type of flexible plantar pressure distribution sensor is used to collect plantar pressure distribution, EMG signal is collected by physiological signal front-end, and motion signal is collected by IMU module. All the data are transmitted to the local mobile terminal through the Bluetooth module. Then the application will upload the evaluation data to the cloud platform for the therapists to check and modify the training plans.

The hardware of the system is mainly divided into five modules: signal acquisition module, a signal processing module, signal transmission module, power management, and a charging module. The signal acquisition module consists of three parts: a

piezoresistive matrix composed of Veloster material, a plantar pressure signal acquisition unit with HC4051 analog multiplexer, an instrument amplifier to complete the acquisition of surface EMG signals and a motion sensor unit based on MPU9250. The signal processing and sending module are composed of MSP430 MCU and FSC-BT822 Bluetooth dual-mode module. The power supply module consists of lithium-ion battery, BQ24610 charging unit and voltage stabilizing unit. The working principle of the system is as follows: the MCU receives data from IMU through SPI communication protocol, collects sEMG and plantar pressure data and preprocesses them. Finally, the above sEMG signal, motion signal, and plantar pressure signal are transmitted through Bluetooth. The data collected from our hardware is then sent to the host computer.

The multifunctional band is an unobtrusive and wearable front end of the wearable multimode system. It's made up of the multifunctional band and a plantar pressure sensor. The main processing module, communication module, and rechargeable Li-battery power supply module were embedded in the multifunctional band with an inertial measurement unit (IMU, Invensense MPU9250) module and an sEMG module with carbonized foam electrode. The novel plantar signal module is connected to the multifunctional band through Flexible Printed Circuit (FPC) cable. The structure of this band and plantar pressure distribution sensor are illustrated in Fig 3.8.

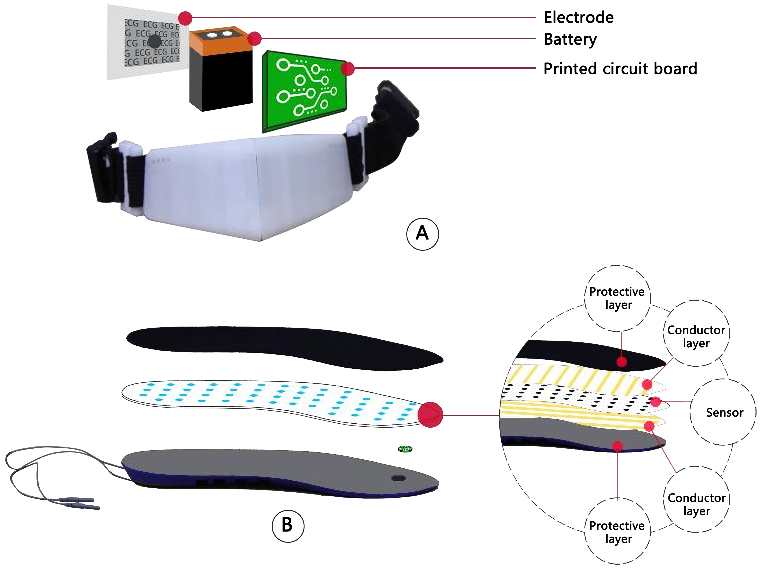

Fig 3.8 (a)Structure of multifunctional band (b) Structure of plantar pressure distribution sensor

The plantar signal module contains two parts, the IMU sensor for plantar motion detection, and a novel plantar pressure distribution insole. We use Velostat, a new pressure-resistance material, to develop a flexible pressure sensor with a novel structure. Furthermore, flexible conductive lines and fabric materials were employed to develop the plantar pressure sensor. The novel structure of this sensor is shown in Fig. 3.8(b).

3.4.1 Plantar pressure acquisition unit

To be specific, a sensor array with 16 rows and 4 columns is used to acquire the high-resolution pressure distribution. The vertical and horizontal conductive lines together with the MCU and resistances put the flexible pressure sensor in a circuit. To minimize the number of ADC ports on-chip, a 16-channel analog multiplexer CD74HC4067 is used in the circuit. The schematic of the plantar pressure distribution insole circuit is displayed in Fig 3.9. Four flexible conductive lines in the upper layer are controlled by the General Purpose Input Output (GPIO) of MCU, and they are set

to Vcc successively to have four loops for the lower layer to acquire the pressure on each flexible pressure sensor.

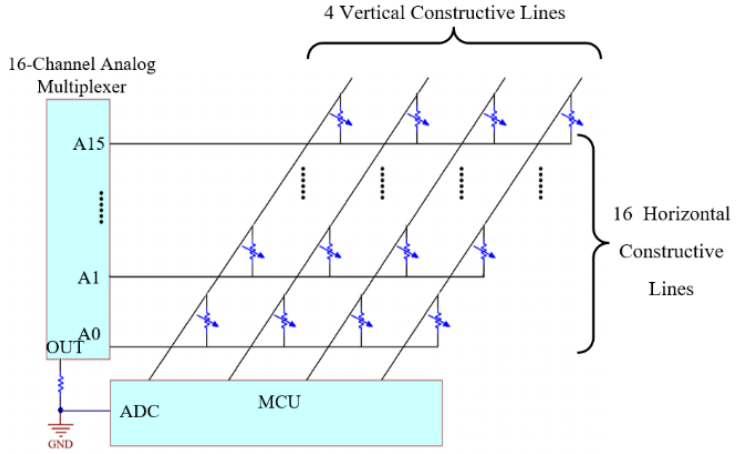

Fig 3.9 Schematic of plantar pressure distribution insole circuit

During the time of choosing a row of electrode signals, the Vcc is connected by the upper analog switch in order. In this way, the 1-10 horizontal lines are selected sequentially. Each time, the 1-5 AD converter works in turn, thus completing the whole sampling process. The circuit diagram of each sample point scanned is shown in Fig 3.10.

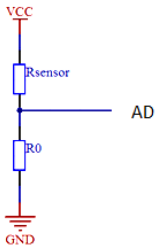

Fig 3.10 circuit diagram of a single sampling point

Therefore, the voltage collected at each sampling point is (3-1):

$$V_{sample} = \frac{R_0}{R_{sensor} + R_0} \times Vcc \tag{3-1}$$

By this method, only 15 electrodes are needed to scan and can collect 10*5 matrix data. At the same time, only one analog switch chip is needed, which improves the efficiency of the IO port and takes into account the spatial layout. The structure diagram of the whole intelligent insole is shown in Fig 3.11.

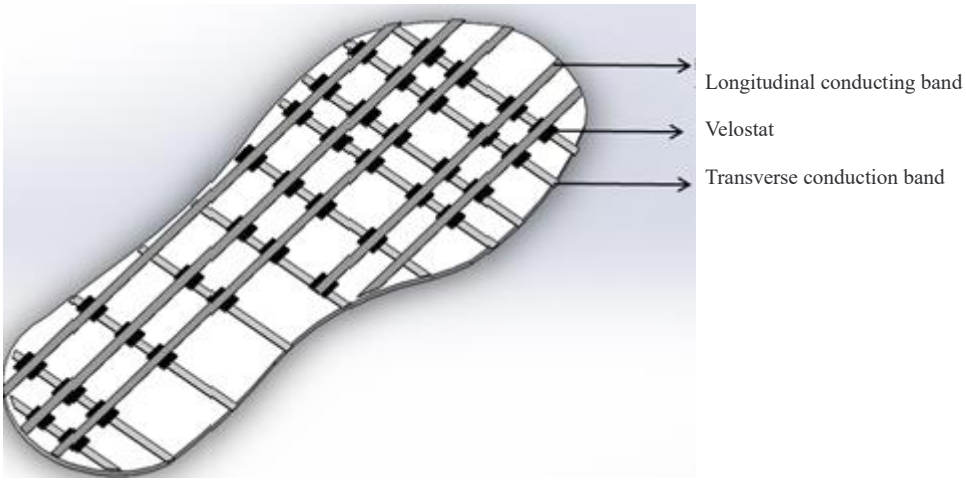

Fig 3.11 schematic diagram of intelligent insoles

3.4.2 Signal processing module

(1) Application architecture

The program is composed of the main program occupying the kernel and the timer interrupt service program, which can realize many tasks such as timing sampling, timing sending, data communication, sensor array scanning and so on. Several tasks are performed sequentially in timer interruption by means of a supercycle. Under the normal working condition of hardware, the task of sampling, filtering, and sending can be executed separately under the design idea of the super-cycle. The sequential execution of each function has no influence on each other, that is to say, the real-time performance of the system is guaranteed. At the same time, the design method has strong program readability and improves the efficiency of modification and transplantation.

(2) Interrupt Service

The timer interrupt service program completes the sampling and sending operations. Sampling is conducted every 100ms. Before sending, the main program checks whether the sending queue has been filled out. If the sending queue has been filled out, the DMA sending program will be started, and the data will be filled out automatically from the sending queue to the UART and sent to the register.

The designated length data is sent to the serial port sending register by DMA_0 channel once, and the rising edge of the interrupt flag bit is triggered by the serial port sending. Enter the DMA interrupt service function after a single transmission is completed. The task of this function is to change the DMA_Done flag bit to 1 in order to inform the main program that the transmission has been completed.

3.4.3 Signal sending module

Data is sent from serial port in the form of the data packet, and the transmission rate of the data packet is 10Hz. The set of data packages is shown in Table 3.2.

Table3.2 packet format

frame header		frame size	Data (n Byte)					check bit
HEAD_H	HEAD_L	LENGTH	DATA0	DATA1	…	DATA(n-2)	DATA (n-1)	CHECK

Fixed-length packets are adopted, each packet is 110 bits. HEAD_H=0x88, HEAD_L=0x74，LENGTH =110（0x6E）CHECK used for odd-even check and come from the xor operation from former 109 bits. The data segment format is shown in the table below, in which table (a) is the acceleration along x, y and Z axes and angular

velocity along x, y and Z axes of two IMUs, and quaternion. Table (b) is the pressure value and EMG signal of the sampled plantar pressure acquisition unit. Among them, the first IMU is placed in the insole, and the second IMU is fixed on the leg.

ACCEL_X, Y, Z are the acceleration values of each axis of the motion sensor, GYR_X, Y, Z are the angular velocity values of the motion sensor around each axis, and Q_0, Q_1, Q_2, Q_3 are quaternions.

Table3.3(a) The format of data segment

Data bits	0-1	2-3	4-5	6-7	8-9	10-11	12-13	14-15	16-17	18-19
Data	ACCEL0_X	ACCEL0_Y	ACCEL0_Z	GYR0_X	GYR0_Y	GYR0_Z	Q0_0	Q0_1	Q0_2	Q0_3

20-21	22-23	24-25	26-27	28-29	30-31	32-33	34-35	36-37	38-39
ACCEL1_X	ACCEL1_Y	ACCEL1_Z	GYR1_X	GYR1_Y	GYR1_Z	Q1_0	Q1_1	Q1_2	Q1_3

Table 3.3(b) The format of the data segment

PRES_s the voltage value of the sampling point of the wheel

Data bits	40-41	42-43	44-45	…	98-99	100-101	102-103	104-105
Data	PRES_1	PRES_2	PRES_3	…	PRES_30	PRES_31	PRES_32	EMG

The data transmission rate of system: serial port baud rate is 115200 and thus transmission rate can reach 10 packages/s, which is 2200 byte/s.

3.5 System Prototype

The prototype of the proposed wearable multimode system is shown in Fig 3.8(a), a plantar pressure distribution sensor can be seen in Fig 3.8(b), printed circuit board(PCB) inside the multifunctional band is shown in Fig 3.12.

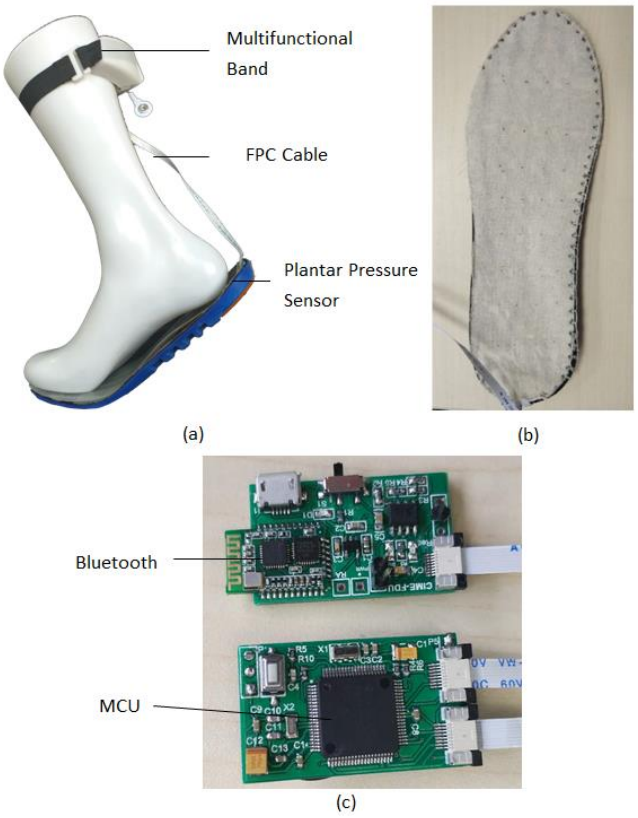

Fig 3.12 (a)Prototype of proposed wearable multimode system (b) Prototype of plantar pressure distribution sensor (c) PCB inside the multifunctional band

We use the instrumentation amplifier to build a physiological signal front ends with a novel carbonized foam electrode to gather the signal of EMG. The analog output of the EMG module is converted to a digital signal by an on-chip 12-bit high accurate Analog-Digital Converter (ADC) in MCU. The use of a carbonized foam electrode will reduce the with less power line interference compared with Ag/AgCl. Fig 3.13 shows the carbonized foam electrode and the EMG module of the proposed system.

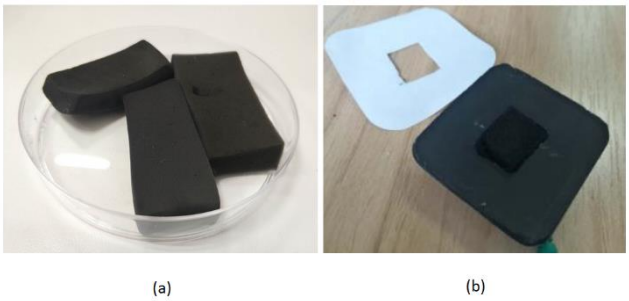

Fig 3.12 (a) Carbonized foam (b) Carbonized foam electrode

Overall, there are two IMUs in this system. One is set under the plantar pressure sensor as presented above, and the other is in the multifunctional band, We collect tri-axis acceleration and tri-axis angular rate from them. The IMU automatic calibrates the tri-axis angular rate by subtracting the offset calculated from the average value of the first 3 seconds when powered on, and the tri-axis acceleration doesn't need to be calibrated under the proposed scenario. These motion signals from these two sensors are transferred to MCU MSP430 in the multifunctional band via Serial Peripheral Interface (SPI).

All the signals from these three modules are collected and processed with the management of MCU. The signal processing procedure includes filtering and data packing. These algorithms will make the local mobile terminal have a better signal quality and to reduce the transmission bandwidth simultaneously. Then, the packaged data are sent to the local mobile terminal synchronously via Bluetooth module, we choose FSC-BT822, whose default UART Baud rate is 115.2Kbps and can support from 1200bps up to 921Kbps. In our system, each data package takes 174 bytes and we send 10 packages per second, which means we need 1740 bps.

Fig 3.13 The illustration of the system in using

3.6 Software Application

The collected data are transmitted to the local mobile terminal. For the evaluation mode, users and their therapists can view the collected foot signals through the software installed in the mobile terminal, which is shown in Fig 3.14. The software displays the waveforms of the EMG signal together with the real-time ankle angle and the plantar pressure distribution. The left part of the application is the training example video for a specific training movement. The right part of the application is the real-time movements capture the display of a patient. Patients should follow the instruction video for certain exercises. A rehabilitation score will be shown on the screen for the precision of rehabilitation.

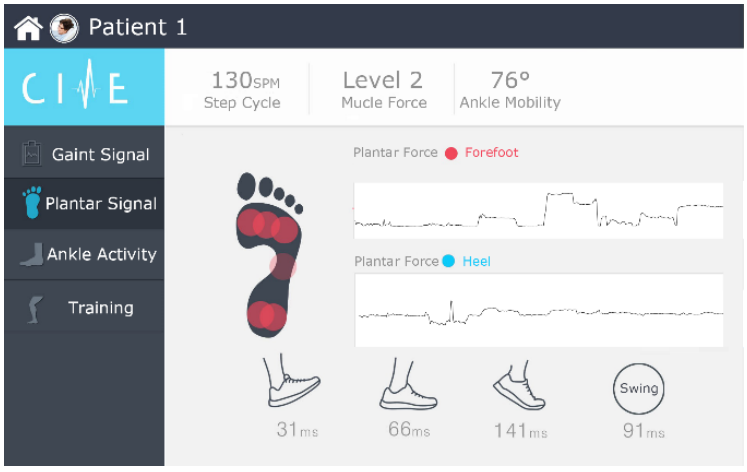

Fig 3.14 User interface of evaluation mode

The proposed multifunctional band together with the plantar pressure distribution sensor was worn to have a whole test of each module and verify their performance, including the signal quality and accuracy test of plantar pressure distribution, EMG signal and motion signal measurement.

3.7 Key formula and algorithm design

3.7.1 Coordinate correction algorithm

The coordinate system of MPU9250 is called s system, and its three axes are Xs, Ys, and Zs respectively. In the course of movement, the S-system will continue to rotate. In order to use the 9-axis inertial sensor to calculate conveniently, it is necessary to rotate the S-system back to the n-system (natural coordinate system). The rotation matrix based on the Euler angle is adopted. Euler angle is a set of three independent angle parameters used to independently determine the position of the rigid body. It consists of pitch angle_, rolls angle_and yaw angle_. The rotation matrices obtained by using Euler angles from s to N systems are as follows (3-2):

$$T_n^s = \begin{bmatrix} c_\psi c_\varphi & s_\psi c_\varphi & -s_\varphi \\ c_\psi s_\psi s_\theta - s_\psi c_\theta & s_\psi s_\psi s_\theta + c_\psi c_\theta & c_\psi s_\theta \\ c_\psi s_\varphi c_\theta + s_\psi s_\theta & s_\psi s_\varphi c_\theta - c_\psi s_\theta & c_\varphi c_\theta \end{bmatrix} \tag{3-2}$$

In the formula, c_ψ, c_φ and c_θ are sinusoidal functions of pitch angle, roll angle yaw angle respectively.

The acceleration of three axes in MPU9250 output s system is named ax_g, ay_g, and az_g respectively. The sensor outputs Euler angles at the same time to construct the selection matrix of the system. The pitch angle of the system is AngleYdeg, the roll angle of the system is AngleXdeg, and the yaw angle of the system is AngleZdeg.

Every moment has an angular velocity matrix and a systematic Euler angle matrix from which the acceleration information of three directions in n system can be extracted for subsequent processing.

3.7.2 Range of motion algorithm

For the measurement of dorsiflexion and metatarsal flexion of the human ankle joint, it is necessary to establish an appropriate ankle joint motion model without considering factors such as muscle contraction and deformation. In addition, the ankle rotation can also be neglected in the evaluation of the joint activity. Therefore, the human ankle joint is simplified as shown in Fig 3.15 below. Two-link model. When evaluating the range of motion of rehabilitation patients, the tibia and sole of the lower leg are abstracted in one plane. The reference range of dorsiflexion is 20 ~30 and the reference range of plantar flexion is 40 ~50.

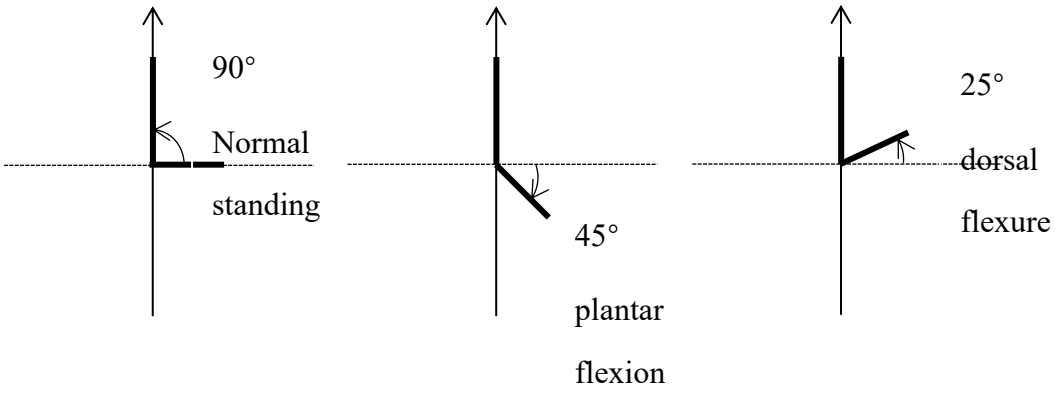

Fig 3.15. A two-link model of human ankle joints

$$w_x = \frac{q_1}{\sqrt{1-q_0^2}} w_y = \frac{q_2}{\sqrt{1-q_0^2}} w_z = \frac{q_3}{\sqrt{1-q_0^2}} \tag{3-3}$$

Where q_0, q_1, q_2, q_3 is the quaternion calculated by MCU. X type, w, w a y, w z is the Angle of the three directions in fig 3.16.

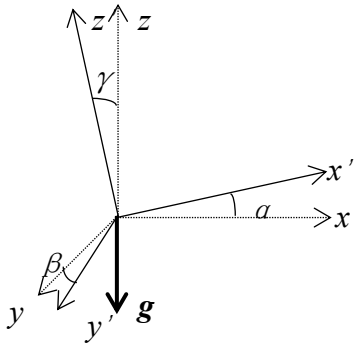

Fig 3.16 schematic diagram of rotation Angle

3.7.3 Gait Period

In normal gait, the time from one heel or toe landing to the other heel or toe landing is called a walking gait cycle. A complete gait cycle is divided into the first touching, supporting and swinging stages, each stage corresponds to different gait periods. The reciprocal of the gait cycle is the step frequency. In order to get the step frequency of rehabilitation patients, it is necessary to divide the acceleration signal into periods.

3.7.4 walking distance

In this system, the step distance is calculated by the kinematics principle. For horizontal acceleration a_x (t) and a_y (t), if the initial velocity of horizontal motion is 0, then there are two kinds of acceleration, one is acceleration a_x (t) and the other is acceleration a_y (t).

$$x(\mathrm{t}) = \sum_{i=0}^{n-1} \sum_{i=0}^{n-1} a_x(t_i)(t_{i+1}) - t_i) \tag{3-4}$$

In the formula, a_x (t) is a function of the acceleration in the direction of X and Y changing with time, and X (T) is the moving distance in the direction of X.

3.8 Evaluation and conclusion

3.8.1 Plantar pressure distribution measurements

Regarding the plantar pressure distribution, we ran the tests on the corridor, as is shown in Fig 3.17(a). We tested the normal walking periods, which mainly include three stages: initial contact, mid-stance and initial swing. So we recorded the data of the plantar pressure sensor and then visualized it in MATLAB using the CUBIC interpolation method. The results can be seen in Fig 3.17 (b) (c) (d) as below. It shows the corresponding pressure images which represent the system can capture the plantar pressure distribution data.

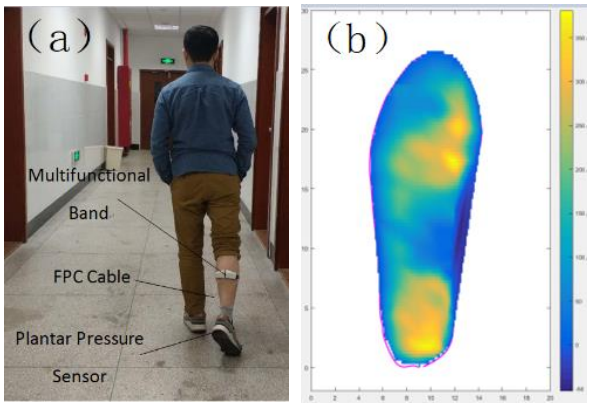

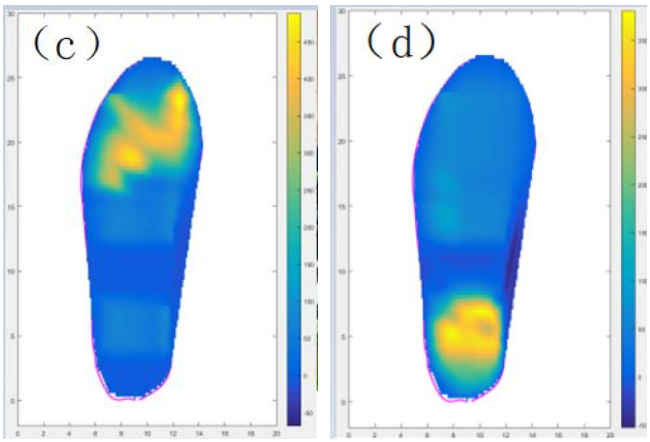

Fig 3.17 Illustration of plantar pressure distribution experiment (b) mid-stance (c) initial swing (d) initial contact

3.8.2 EMG signal measurement

Experiments on lower limb motion were designed to validate the EMG module of our system. We tested the motions of normal walking and stamping the ground, and carbonized foam electrodes were put on the calf muscle and the results are shown in Fig 3.18. The waveform of EMG signals shows this module can measure whether a certain muscle or a muscle group is active when a patient does a specific motion.

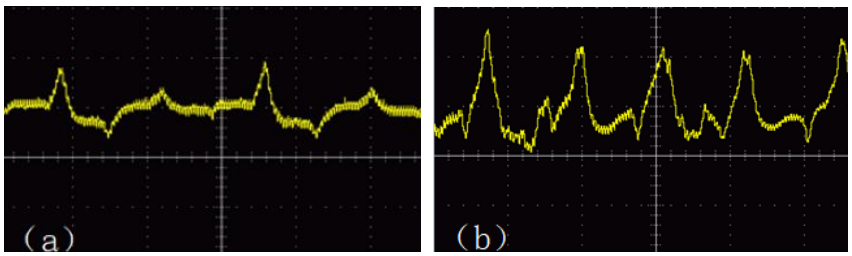

Fig 3.18 EMG waveforms under: (a) normal walking (b) stamping ground

3.8.3 Motion signal measurements

For the test of ankle mobility, we used video information to compare with the proposed system, as shown in Fig 3.19. We recorded the video of a subject doing ankle dorsiflexion and plantar flexion, then calculated the ankle mobility on the computer. From the video, the maximal angle for the subject's ankle motion is 61.8°, while the result from our system is 65.2 °, then the error percentage is 5.5%. This error rate is acceptable because the IMU may have some fluctuation.

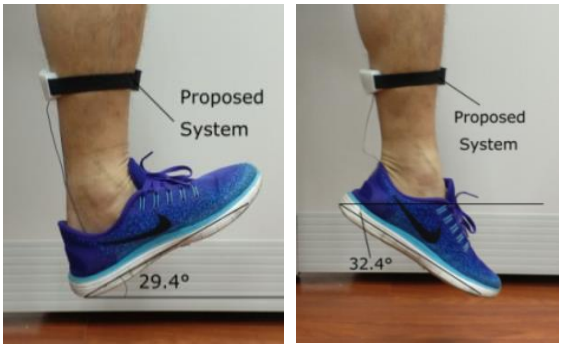

Fig 3.19 Screenshots of the video for ankle mobility

3.9 Discussion and Conclusion

In this part, a novel wearable multimode system using soft sensors for lower limb activity evaluation and rehabilitation systems with flexibility and modularity is proposed. Patients can get lower limb activity evaluation in home-based scenarios and rehabilitate with the training plan given by therapists through the Internet using the proposed system's software. Compared with the current clinical practice, this proposed system will reduce the cost of the rehabilitation process and bring convenience for the patients. Also, the therapists can get access to the rehabilitation status of different patients using the cloud platform in this system and give a more efficient training plan.

The novel soft carbonized foam electrodes are embedded in the proposed system to obtain an EMG signal and a novel flexible plantar pressure distribution sensor is also used in this system. All the sensors and electrodes are all unobtrusive for the patients' daily life. The multimode design of this system can also make the system suitable for different patients.

More clinical trials are needed to evaluate the performance of the algorithms, system endurance, and sensibility under different rehabilitation circumstances. Detailed analysis and optimized algorithms will be studied based on this system. The system has some reserve ports for the further development of different sensors, such as galvanic skin response (GSR) signal. These additional sensors will provide modalities of monitoring parameters. And data fusion techniques will be explored with more clinical data. Also, Some self-adaption networks will be used in the algorithms as well.

4 Convolutional Neural Network for Parkinsonian Gait Recognition and Classification using Surface Electromyography

Parkinson's disease (PD), as a common neurodegenerative disorder, has primary manifestations like movement poverty, muscle rigidity, gait disturbances, etc. Recognition of Parkinsonian gait patterns is helpful in the diagnosis of PD and establishing effective therapies. In this thesis, a Convolutional Neural Network (CNN) and surface Electromyography (sEMG) based Parkinsonian gait (PG) recognition system is proposed. Two-channel sEMG signals were obtained from gastrocnemius muscle and tibial anterior muscle at the shin. Then these signals were passed to CNN after filtering and time-series segmentation. The system omits the complex hand-crafted feature extraction process. Meanwhile, two CNN models, namely, generic model and subject-specific model were built and validated on a dataset that was collected from eleven volunteers. The accuracy of the proposed system for distinguishing the Parkinsonian gait from normal or other pathological gaits can reach 90% for the generic model, and 97% for the subject-specific model. With the high accuracy in identifying the PG, the proposed system can be extended as a promising aid tool in discriminating PG from normal gait and pathological gaits.

4.1 Introduction

PD is a common neurodegenerative disorder of unknown cause that occurs in adults, whose clinical hallmarks are movement poverty and slowness, muscle rigidity, limb tremor or gait disturbances and as called, parkinsonian gait[31]. Although PD is common in the clinic, it’s still difficult to diagnose, mainly relies on the medical history, physical examination and signs after dopamine supplementation treatment[30]. These examinations heavily depend on the experience of doctors, and

can not reflect the development of PD and the neuromuscular function in dynamic activities. Acting as a portrayal of people's physical behavior, gait analysis has been widely used in rehabilitation treatment, disease prediction and clinical aspects[32].

sEMG is a comprehensive effect of superficial muscle EMG and nerve trunk electrification on the skin surface, at present, many scholars have begun to use sEMG to evaluate the neuromuscular status and motor function of PD patients. A.I.Meigal et al.[33] evaluate a variety of traditional and novel sEMG characteristics of biceps brachii muscle in patients with PD and compare the results with the healthy old and young control subjects to evaluate the potential of the parameters in the assessment of the severity of PD. On the other hand, PD patients always show abnormal gait, so it’s of great clinical value and social significance to explore the gait characteristics from sEMG in the dynamic activities of PD patients. Julien Stamatakis et al.[34] proposed a low-cost Gait feature extraction method for the application of PD, which could quantify the Gait asymmetry and FOG (Freezing of Gait) more deeply and improve the accuracy, such study may be beneficial to guide clinical treatment and improve the diagnostic accuracy of PD.

Traditional gait analysis methods are mainly based on the video, pressure sensors or large gait simulation platform, while with the improvement of computer power, deep learning technology, especially CNN has dramatically improved the state of the art in medical applications. Esmaeilzadeh et al.[35] applied a deep learning framework for simultaneous classification and regression of Parkinson's disease diagnosis based on MR-Images and personal information. Wei Yuan et al.[36] proposed a CNN based gait classification method from mobile phone built-in accelerometer and overall classification accuracy can reach over 90%. While before training the raw data need to be transformed into image firstly, which increased the complexity of the method.

To our best knowledge, using neural networks without the complex feature extraction process for the sEMG of PD has seldom been explored.

In this thesis, sEMG and deep learning-based framework for identification of the PD gait is proposed. Two-channel sEMG signals from gastrocnemius muscle and tibial anterior muscle were collected and passed to a six-layer CNN after filtering and time-series segmentation. As a preliminary study to distinguish normal gait, PG and other pathological gaits, both subject-specific models and generic models were established and validated. With the help of neural networks, the proposed system doesn't require the complex hand-crafted feature extraction process and shows great potential in clinical assistant diagnosis, illness-early-warning and guardianship in-home.

4.2 Method

4.2.1 Data acquisition experiment setup

Basic pathological gaits that can be attributed to neurological conditions include hemiplegic, sensory, neuropathic, spastic diplegic, choreiform, myopathic, ataxic (cerebellar) and Parkinsonian. In clinical research, besides parkinsonian certain pathological gait are more likely to encounter, some typical representatives are neuropathy-related pathological gait like hemiplegic gait, spastic diplegia gait and steppage gait, and also some other pathological gait like gluteus medius gait and gluteus maximus gait.

During free ambulation, patients with PD demonstrate shorter stride length and walking speed while double support duration and cadence rate are increased[37]. They have difficulty starting, but also has difficulty stopping and this is due to muscle

hypertonicity. In this study, we established an sEMG based dataset of simulated PG, in which more than 60 thousand segments sEMG data of natural gait and simulated pathological gait were collected from 11 subjects. The sEMG data of gaits were measured by the Shimmer3 EXG unit, which is a small and robust wearable wireless sensor created by Realtime Technologies Ltd and offers good data quality.

Experiments were conducted on 11 subjects (eight males and three females). To test the recognition ability of the proposed neural network, besides PG we added hemiplegia gait, gluteus medius gait, and steppage gait as supplementary. Each subject was asked to imitate PG and another one kind of pathological gait among them in addition to normal gait. The height of subjects ranges from 163cm to 191cm with a mean value of 173.5cm, the weight of subjects ranges from 48kg to 93kg with a mean value of 65.8kg. Table 4.1 shows the detail information of subjects.

Table 4.1 The Detailed Information of Subjects

No.	**gender**	**Height(cm)**	**Weight(kg)**	**pathological gait besides Parkinson**
1	male	191	93	hemiplegic gait
2	male	170	70	gluteus medius gait
3	male	168	60	steppage gait
4	male	176	55	hemiplegic gait
5	male	165	62	gluteus medius gait
6	female	168	56	steppage gait
7	male	185	62	gluteus medius gait
8	male	180	82	hemiplegic gait
9	male	174	77	steppage gait
10	female	168	59	gluteus medius gait
11	female	163	48	hemiplegic gait

(1) Learn and train to simulate pathological gaits

For the learning of PG and the other three kinds of pathological gaits, every subject was instructed to watch and study the Stanford Medicine 25 video which was created in conjunction with Stanford's AIM lab to teach the examination of the gait[38].

(2) Collect the natural and pathological gait information

The Shimmer3 EXG unit is fixed to the outer part of two shins by an elastic bandage, wherein the two channels of sEMG were placed on the abdomen of the gastrocnemius and tibialis anterior muscle respectively, ankle bone was chosen as the reference since reference electrode should be placed at an electrically neutral point of the body. The distance between the two electrodes of each channel was set as 4cm and the reference electrodes were attached to the skin of the lateral malleolus fibula. Set the sampling rate of the system to 512Hz, then the subjects were asked to walk normally on a straight horizontal cement alleyway and make sure the number of steps was bigger than 100 to get enough data. sEMG of left and right lower limbs under natural gait are obtained then. Figure 1 shows the placement of the Shimmer3 EXG unit and the sEMG electrodes.

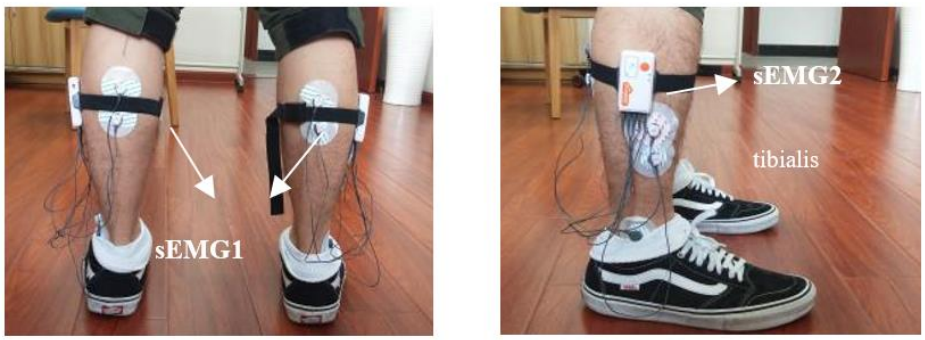

Fig 4.1 Placement of EXG unit and sEMG electrodes. (a) Back View (b) Side View.

Fig 4.2 shows the sEMG's linear envelope of PG and other selected three kinds of pathological gaits (20s per segment), where we can see a more disorderly pace.

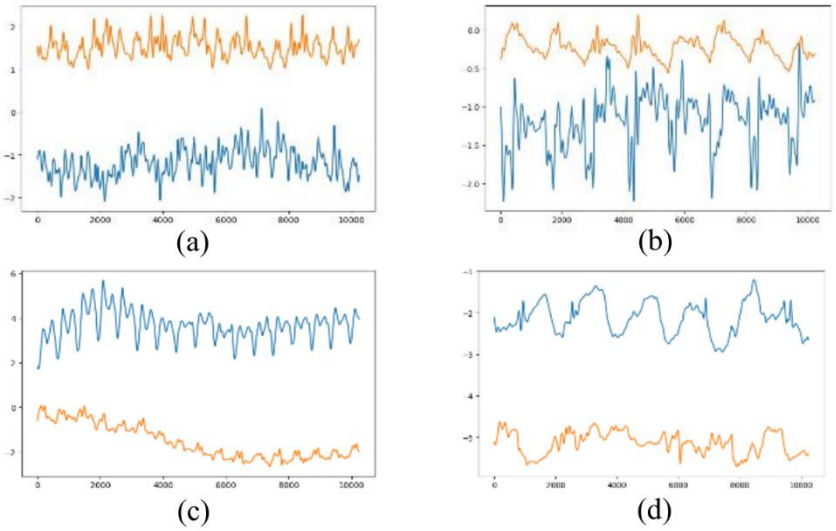

Fig 4.2 The sEMG's linear envelope of (a) Parkinsonian gait (b) hemiplegic gait (c) gluteus medius gait (d) steppage gait

4.2.2 Dataset preparation

The ADS1292R chips on the EXG Unit provide a DC-coupled measurement. To detect when a muscle is active and to give an indication of the overall level of activity in a particular muscle the linear envelope of EMG signal was extracted. Meanwhile, since the sensor is very sensitive, many noises are introduced thus may cause the overfitting of neural network and in view of normal stride frequency of adult range from 0.5 Hz to 3 Hz roughly, a third-order low-pass Butterworth Filter is designed and used. The normalized cut-off frequency $W_N = 2 * f_{cut-off}/f_{sample}$ was set as 0.02, where $f_{cut-off}$ is the raw cut-off frequency and f_{sample} stands for our sampling rate, 512Hz.

We use a sliding sequential segmentation window with 1024 points long (which is, 2000ms in time series under a sampling rate of 512Hz) and 256 points stepping to segment the waveforms into fragments of 2000ms. Each segment contains 2*1024=2048 points, wherein the 2 here are two channels of sEMG which collected from the gastrocnemius and tibialis anterior muscle respectively. And all the two adjacent fragments overlap each other by three quarters after this process. Fig 4.3 shows 5 segments of data each, where (a) is a raw sEMG linear envelope and (b) shows the filtered signal.

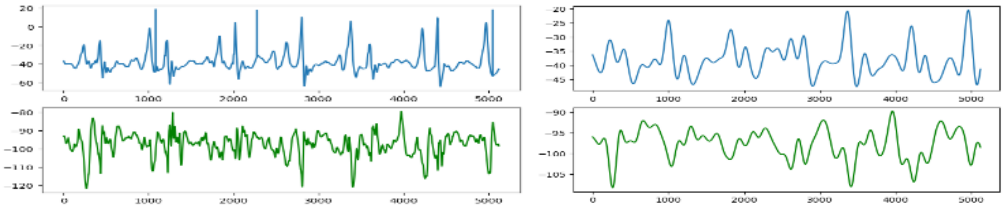

(a) (b)

Fig 4.3 (a) Raw SEMG linear envelope (b) Filtered SEMG linear envelope

Meanwhile, all fragments are labeled according to the gait category to obtain the (data, label) pair. The labels are set as 0 for the subject's simulated pathological gait, 1 for hemiplegic gait and 2 for Parkinson's gait.

4.2.3 Neural network build-up and training

Neural Networks can work as a kind of classification system. Inspired by biological neural networks of human brains, it's a framework for many different machine learning methods rather than an algorithm, and has advantages in processing complex data inputs. CNNs are a category of Neural Networks that have proven very effective in areas such as image recognition and classification. CNN was built and trained in this section to explore its performance in this PG recognition and classification task.

(1) Structure

CNNs are a category of Neural Networks that have been proved to be very effective in image recognition and classification. Lenet is one of the earliest convolutional neural networks, which promotes the development of deep learning. Yann Lecun's pioneering work was named lenet5 after many successful iterations. In image recognition tasks the nearby pixels typically have a strong relationship with each other, and similarly, for our study, the nearby acceleration readings are likely to be correlated in the given data fragments. Thus LeNet-like CNN is chosen as the third model to build in this study.

In image recognition tasks the nearby pixels typically have a strong relationship with each other, and similarly, for our study, the nearby sEMG readings are likely to be correlated in the given data fragments. Thus LeNet-like CNN is chosen as the model to build in this study.

A six-layer CNN was defined for PG recognition and classification. They are convolution layer one whose values are fixed by the input data, pooling layer 1, convolution layer 2, pooling layer 2, the hidden full connection layer and the softmax output layer whose values are derived from previous layers. Wherein, each layer is fully connected to the next layer.

Figure 4.4 demonstrates the structure of CNN in this study. As mentioned before, the shape of input data is (1,2,1024), the shape of convolutional output1 is (16, 28, 28) with 16 convolutional kernels of size 4 and the shape of max-pooling output 1 is (16, 14, 14) with pooling size of 2 and strides of 2. Similarly, the shape of convolutional output 2 is (16, 14, 14) and the shape of max-pooling output 1 is (16, 7, 7). The dimension of two fully connect layers is 300 and 3, respectively. The output layer is a Softmax classifier.

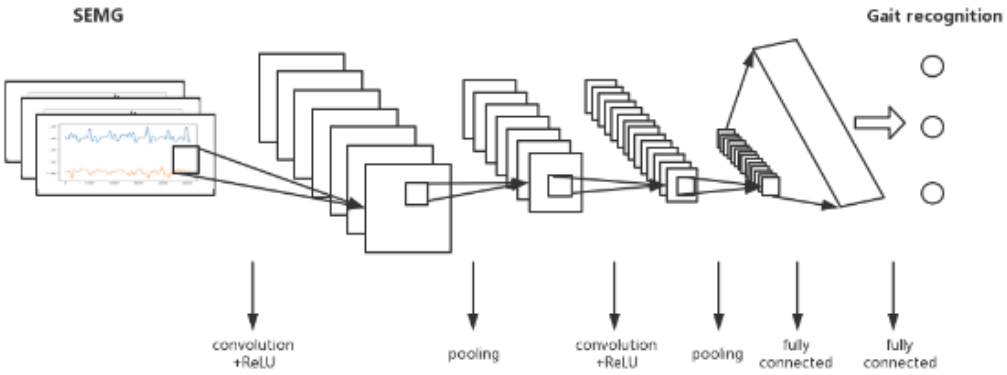

Fig 4.4 The structure of CNN for PG Recognition and Classification

The activation function of the hidden layer is ReLU (Rectified Linear Unit) to introduce non-linearity in our net, and its formula is given by (4-1).

$$f(x) = max\ (0, x) \tag{4-1}$$

Other nonlinear functions such as tanh or sigmoid can also be used instead of ReLU, but ReLU has been found to perform better in these situations.

By using softmax as the activation function, the sum of output probabilities from the output layer is 1. The softmax function can take a vector of arbitrary real-valued scores and squashes it to a vector of values between zero and one. Here it's given by (4-2).

$$P(y = j|x) = e^{x^T w_j} / \sum_{k=1}^{3} e^{x^T w_j} \tag{4-2}$$

Where w_j(j＝0,1,2) here represents the weight vector from the hidden layer to the output layer.

(2) Cost function and optimization algorithm

A cost function is needed to optimize the weights of each node during training. In multi-classification tasks, mean square error (MSE) is usually used as the basic kind of cost function. While in the process of training the neural network, we update the node weights W and node output B by gradient descent algorithm, so we need to calculate the derivative of the cost function to W and B, but the update may be very slow in this process. To overcome this cross-entropy cost function is chosen as the cost function, it's formula is given by (4-3):

$$\mathrm{C} = -\frac{1}{n}\sum_{x}[yln\ a + (1-y)\ln(1-a)] \tag{4-3}$$

Where y is the expected output and $\mathrm{a} = \sigma(\sum W_j * X_j + b)$ is the actual output of neurons.

Meanwhile, to prevent overfitting and improve the generalization ability of our neural network, and L2 regularization was added into the cost function, thus the lost function becomes (4-4):

$$\mathrm{L} = C_0 + \frac{\lambda}{2n}\sum_{w} {w_j}^2 \tag{4-4}$$

Where C_0 stands for the former cost function, n is the size of the training set and λ is the regularization parameter.

The optimization algorithm is set as Adam optimizer that combines the advantages of both the AdaGrad and RMSProp optimization algorithms. The gradient update formula is (4-5):

$$\theta_t = \theta_{t-1} - \alpha * \widehat{m_t}/(\sqrt{\widehat{v_t}} + \varepsilon) \quad (4\text{-}5)$$

Where the default learning rate α is set as 0.001, $\varepsilon = 10^{-8}$ just in case the dividend is zero. m_t stands for gradient mean:

$$m_t = \beta_1 m_{t-1} + (1 - \beta_1) g_t \quad (4\text{-}6)$$

and v_t stands for gradient variance (4-7).

$$m_t = \beta_1 m_{t-1} + (1 - \beta_1) g_t \quad (4\text{-}7)$$

Where β_1, β_2 is exponential attenuation rate, g_t is the gradient at time t.

4.2.4 Training Process

The training of neural networks we built in this study follows the typical process and weight updating rules. To take a general exposition the pseudo-code for the PG recognition CNN model is described in Algorithm 4.1 below.

Algorithm 4.1: CNN for Parkinsonian Gait recognition and classification

---

Input: Labeled train dataset D = {((x_i, y_i, z_i), L_i)}, an unlabeled dataset D(unlabeled) = {(x_i, y_i, z_i)}

Output: gait type Labels L_{pre} of the unlabeled data

Initialization

random assignment weights and biases of the network

Repeat

Forward Propagation:

For each Labeled train data of sEMG from D:

---

do

- Calculate Output of Hidden Layer and Output Layer
- Calculate the deviation between the output layer and the expected output

end

• Use softmax to do classification and update

the weight of each edge in the network

Backward Propagation:

• Conduct backward propagation

Until w_i convergences or training epochs meet n;

Use the trained network to predict the labels

4.3 Results

After preprocessing of the acquired sEMG, we get a labeled dataset $D\{((SEMG1_i, SEMG2_i), L_i)\}$(Li =0,1,2) of 5 types of gait with more than 60 thousand segments. After the shuffle, the dataset was grouped into the training set and the test set with a ration of 0.7. The training set was used to train the model and the test set was used to verify the classification effect of the model when the train finished.

4.3.1 Generic model

In the generic model, CNN is established for a three-class classification task (normal gait, Parkinsonian gait, and other pathological gaits). The node counts of hidden fully connect layer were set as 300, the learning rate was 0.0001 and batch size, which is the number of training samples in each batch, was set as 128. Fig 4.5 shows the confusion matrix and ROC of PG recognition of the model after 24 epochs of training. Where the Precision P = TP/(TP+FP) is the proportion of real positive samples in the

positive samples judged by the classifier, the Recall R = TP/(TP+FN) is the proportion of the true judged positive cases in all positive cases.

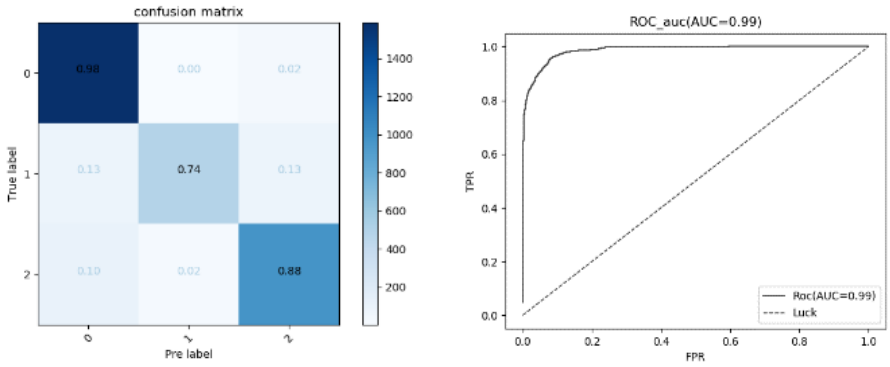

Fig 4.5 The confusion matrix and ROC after 24 epochs of training

ROC (receiver operating characteristic curve) and confusion matrix are used to evaluate the performance of the proposed system. ROC can identify the ability of PG recognition at any threshold value. Confusion matrix, also known as error matrix, is a standard format for accuracy evaluation. From the confusion matrix of the 24th epoch, we can observe that for the PG recognition task, the precision of recognizing different types of gait is 0.98, 0.74 and 0.88 respectively, where the precision is the proportion of real positive samples in the positive samples judged by the classifier. We can calculate the recall value from the matrix as well, which is 0.77, 0.98 and 0.85 respectively, where the recall is the proportion of the true judged positive cases in all positive cases. For PG the recall value is 0.98, far bigger than its precision, this is promising because in practical use scenarios we hope the model can recognize the disease as much as possible, even if the false alarm occurs.

By applying the generic model on the test set, the accuracy can achieve 0.9008. For a generalization model, the result is quite promising and exhibits the feasibility of the proposed system for the PG recognition.

4.3.2 Subject-specific model

To take the individual variability into consideration and to obtain a personalized model for each subject, subject-specific models were obtained. The setting of all parameters remains unchanged. Fig 4.6 shows the confusion matrix and ROC of one of our subjects after 20 epochs of training.

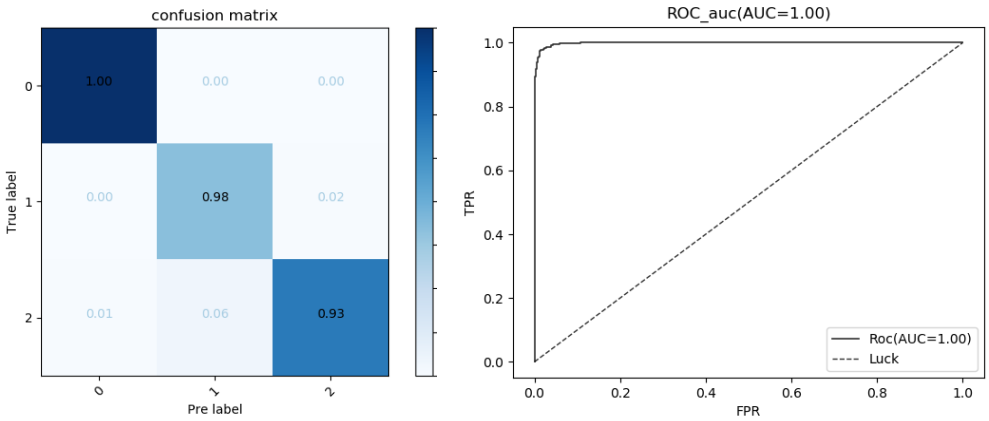

Fig 4.6 The confusion matrix and ROC of subject No.3 after training

Where label 0 stands for NG and 1 stands for PG. We can observe a higher accuracy of 100% for NG and 0.98 for PG. Table 4.1 shows the accuracy score after the training for each subject after training. The accuracy score fluctuates between 0.8361 and 0.9737 with an average value of 0.9282.

Table 4.1. Classification Precision of each subject

No.	Gender	Classification Task	Accuracy Score
1	male	{NG[a],PG[b],hemiplegic gait}	0.8786
2	male	{NG,PG,gluteus medius gait}	0.9732
3	male	{NG,PG,steppage gait}	0.9512
4	male	{NG,PG,hemiplegic gait}	0.8979
5	male	{NG,PG,gluteus medius gait}	0.9692
6	female	{NG,PG,steppage gait}	0.9398
7	male	{NG,PG,gluteus medius gait}	0.9712
8	male	{NG,PG,hemiplegic gait}	0.8361
9	male	{NG,PG,steppage gait}	0.9737
10	female	{NG,PG,gluteus medius gait}	0.9686
11	female	{NG,PG,hemiplegic gait}	0.8510
AVG			0.9282±0.05

[a.] Normal Gait [b.] Parinson Gait

From Table 4.1, for the three-class classification task {normal gait, PG, hemiplegic gait}, the average accuracy is only 86.59%. It is mainly because our dataset combines sEMG signals from two legs, while for hemiplegic patients, one side of the sEMG is affected and the other side may maintain normal. For other three-class classification tasks, the average accuracy can reach over 96%.

4.4 Conclusion

To provide an accurate and affordable measure of PD identification, an automatic PG recognition system based on the sEMG was proposed in this thesis. The signals were fed to CNN for classifying the normal gait, PG and some other pathological gaits. The proposed system omitted the complex hand-crafted feature extraction process.

Experimental results demonstrate the effectiveness of the proposed approach in automatic PG gait recognition. The accuracy of the proposed CNN can reach 90% for all the subjects' generic models and 97% for the subject-specific model. Meanwhile, the results showed that the network works better when trained for a specific subject, which is of great significance in tracking patients' disease stages. To our best knowledge, this is the first work that combines sEMG with CNN for recognition of PG. In the future, larger datasets will be collected in the cooperated hospital to further validate the robustness of the proposed system. Some data fusion technologies like camera + sEMG based PG analysis are also worth pursuing.

5 Neural Networks for Pathological Gait Classification Using Wearable Motion

Gait, as an essential feature reflecting human health status, has attracted extensive attention in research. Automatic pathological gait identification can contribute to disease diagnosis and intervention. In this thesis, an unobtrusive sensing technology with deep learning methods to discriminate healthy and pathological gaits is proposed. Two accelerometers are mounted on the left and right lower limbs to acquire the motion signals. Based on these signals, three Neural Networks, namely, BPNN (Back Propagation Neural Network), LSTM (Long Short Term Memory) and CNN (Convolutional Neural Networks) are proposed for classifying the gaits. Experimental results exhibit that the accuracy of the proposed method can reach 86%, 81%, and 93% on a database of 15 participants while using BPNN, LSTM, CNN, respectively. With the strong ability of spatial-temporal signal analysis, CNN outperforms the other two neural networks and provides a favorable result. The proposed method can be extended to an automated gait classification tool, which can be used in the diagnosis and identification of pathological gaits.

5.1 Introduction

Gait, as the manner of walking, is an idiosyncratic feature of a person. In general, gaits can be classified into normal gait and pathological gaits. The pathological gaits may mainly cause due to hemiplegia, Parkinson's disease, myopathy, and pain. It includes typically gaits, namely, hemiplegic gait, Parkinson gait, gluteus medius gait, steppage gait and so on[39]. Identification of normal/pathological gaits could provide deep insights to understand various human movement patterns across different gait pathologies. It has been proven that gait analysis has a guiding role both in clinical

research and guardianship in-home[40]. However, traditional gait assessment is mainly based on clinical observations. It is a subjective and time-consuming decision-making process for clinicians. To address these issues, automatic methods to discriminate between normal and pathological gaits have been attracted widespread attention.

With the benefits of precise, stable and affordable sensors, various motion sensor-based gait classification methods have been presented. Dolatabadi et al.[41] integrated machine learning methods to discriminate between healthy and pathological gait patterns using the Kinect motion sensor. Gait features are extracted and k-nearest neighbor and a dynamical generative classifier are used. Murad et al.[42] classified pathological gait patterns using 3D ground reaction force (GRFs) data, the GRFs parameters and the discrete wavelet transform (DWT) were used to extract the gait features and nearest neighbor classifier (NNC) and artificial neural networks (ANN) were investigated for the classification of gait features, the result shows the optimal feature set of six features enhanced the accuracy to 95%. In the existing works, by combining the sensor technology and traditional machine learning algorithms, gait classification can achieve high performance in pathological gait classification tasks. However, hand-crafted features are required to be extracted before the classification.

Nowadays, deep neural networks have shown great potential in feature extraction and become a research hotspot. Neural networks have shown their ability in gait authentication[36] and activity recognition[43]. To our best knowledge, using neural networks without the complex feature extraction process for the pathological gait classification has never been explored. With the hypothesis that gait patterns could be captured and compartmentalized via combining motion sensors with neural networks, a novel method is proposed. In this thesis, two wearable motion sensors are used to

acquire the motion signals and ANNs (BPNN, LSTM, and CNN) based pathological gait classifiers are used to identify different gaits. The proposed method omits the complex sensor set-up process and hand-crafted feature extraction process. On the contrary, with the ability to act as feature extractors, the proposed method can learn multiple layers of feature hierarchies and realize the classification automatically.

5.2 Method

5.2.1 Data acquisition experiment setup

In clinical research certain pathological gait are more likely to encounter, they are hemiplegic gait, steppage gait, parkinsonian gait, and gluteus medius gait. For this study, we established a dataset of pathological gait, in which more than 100 thousand segments motion data of natural gait and five simulated pathological gaits were collected. The gait data were measured by Shimmer 3 IMU unit which is a small wearable wireless sensor and can offers data with integrated 9DoF inertial sensing.

Experiments were conducted on 15 subjects and among them 3 are female. The height of subjects ranges from 163cm to 191cm with a mean value of 172.47cm and the weight range from 48kg to 93kg with a mean value of 65.8kg. The steps of the experiment to obtain the needed data are presented below.

(1) Collect motion data of natural gait

The Shimmer 3 IMU unit is fixed to the outer part of two shins by an elastic bandage, wherein the Y-axis of IMU is set perpendicular to the horizontal plane, the X-axis is perpendicular to the human coronal plane, and the Z-axis is perpendicular to the sagittal plane of the human body. We set the sampling rate of the system to 512Hz and set the IMU's accelerometer sensitivity to ±2g, then the subjects were asked to walk naturally

on a straight horizontal cement alleyway and make sure the number of steps was bigger than 100 to get enough data. The triaxial acceleration information of the left and right lower limbs under natural gait is obtained then. Fig 5.1(a) shows the placement of Shimmer 3 and Fig 5.1(b) shows the scene of the experiment during subject walking.

(a) (b)

Fig 5.1 (a) The placement of Shimmer 3 IMU unit; (b) The walking scene.

(2) Learn to simulate five pathological gaits

Since in this study we only use the motion sensor, it's promising to just simulate those pathological gaits instead of collect clinical data to verify the model. For learning those pathological gaits, each subject was instructed to watch and study the Stanford Medicine 25 video which was created in conjunction with Stanford's AIM lab to teach the examination of the gait[38].

(3) Collect pathological gait information

The placement of the IMU and data acquisition process is the same as step 1. Five typical pathological gaits were selected, they are hemiplegia gait, Parkinson gait, gluteus medius gait, steppage gait and diplegia gait (scissor gait).

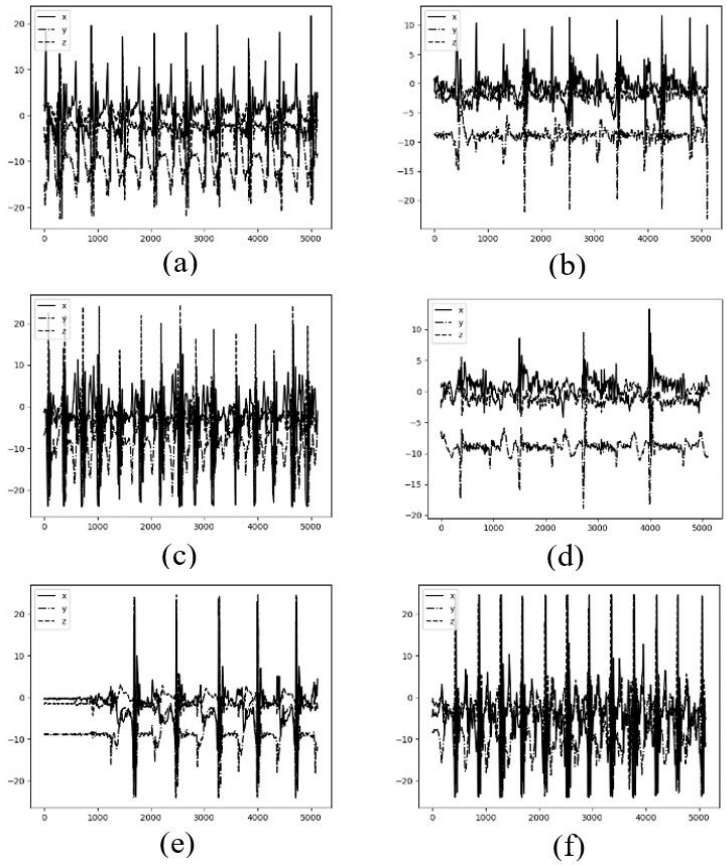

Fig 5.2 (a) natural gait (b) hemiplegic gait (c) Parkinson gait (d) gluteus medius gait (e) steppage gait (f) diplegia gait.

Fig 5.2 shows the original triaxial acceleration data of the natural gait and five pathological gaits (10s per segment), from which we can observe a lower stride frequency and disorderly pace.

5.2.2 Data preprocessing and dataset preparation

Since the IMU is very sensitive, the obtained motion signals are contaminated with noise that may cause the overfitting of neural networks. To reduce this side effect and since normal stride frequency of adults ranges from 0.5 Hz to 3 Hz roughly[44], a third-order low-pass Butterworth Filter is designed and used. The normalized cut-off

frequency $W_N = 2 * f_{cut-off}/f_{sample}$ was set as 0.1, where $f_{cut-off}$ is raw cut-off frequency and f_{sample} stands for our sampling rate, 512Hz.

Then the filtered IMU data is normalized into [-1,1] with zero mean to reduce individual variability. We use a sliding sequential segmentation window with 1024 points long (which is, 2000ms in time under a sampling rate of 512Hz) and 256 points stepping to segment the waveforms into fragments of 2000ms. Each segment contains 3*1024=3072 points where 3 represents the x, y, and z-axis' triaxial acceleration information. Meanwhile, all fragments are labeled according to the gait category to obtain the (data, label) pair.

5.2.3 Neural network build-up and training

Inspired by biological neural networks of human brains, Artificial Neural Network (ANN) is able to recognize patterns and learn features from input data without extensive data preprocessing, handcrafted rules or feature engineering[45], which makes them particularly well suitable for classifying our motion data of gait. To explore a suitable neural network for this Pathological Gait Classification task, we start from the most basic one – back propagation neural network. On the other hand in view of our input data is in time series and RNN is quite good at processing sequential data, we built an RNN to evaluate its classification performance. We also evaluate CNN cause lately, it has dramatically improved the state of the art in medical applications in recent years.

(1) BPNN (backpropagation neural network)

We build up a three-layer BPNN in this part. It's the most basic neural network, whose output results are propagated forward and the error is propagated backward, simple and efficient. The layers are the input layer, hidden layer, and output layer. In our study, the

number of nodes in the input layer was set according to the points in each data fragments, which is 3072 (3 axes * 2000ms * 512Hz). The number of output layer nodes is 6 since we have 6 types of gaits in all. Fig 5.3 shows the structure of our BPNN.

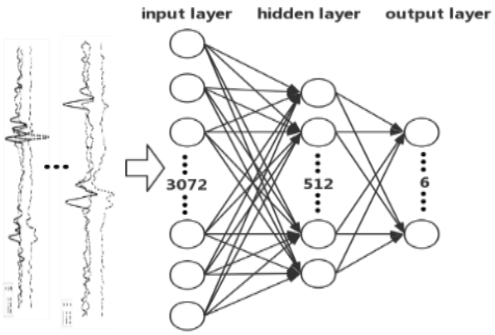

Fig 5.3 The structure of constructed three-layer BPNN

The activation function of the hidden layer is ReLU (Rectified Linear Unit) to introduce non-linearity in our net, and its formula is given by (5-1).

$$f(x) = \max(0, x) \tag{5-1}$$

Other non-linear functions such as tanh or sigmoid can also be used instead of ReLU, but ReLU has been found to perform better in this situation.

The sum of output probabilities from the output layer is 1. This is ensured by using the softmax as the activation function in the output layer and the function is given by (5-2).

$$P(y = j|x) = e^{x^T w_j} / \sum_{k=1}^{6} e^{x^T w_j} \tag{5-2}$$

Where w_j(j＝0:5) is the weight vector from the hidden layer to the output layer.

A cost function is needed to optimize the weights of each node during training. To overcome the slow update of node weights, a cross-entropy cost function is chosen as the cost function, it's formula is given by (5-3).

$$\mathrm{C} = -\frac{1}{n}\sum_{x}[y ln\, a + (1-y)\ln(1-a)] \tag{5-3}$$

Where y is the expected output, n is the number of samples, and (5-4) is the actual output of neurons.

$$\mathrm{a} = \sigma(\sum W_j * X_j + b) \tag{5-4}$$

Besides, to prevent overfitting and improve the generalization ability of our neural network, and L2 regularization was added into the cost function. Thus the lost function becomes (5-5):

$$\mathrm{L} = \mathrm{C} + \frac{\lambda}{2n}\sum_{w} {w_j}^2 \tag{5-5}$$

Where C stands for the former cost function, n is the size of the training set and λ is the regularization parameter.

(2) LSTM (Long Short Term Memory)

LSTM is the enhanced version of RNN (recurrent neural network) that can alleviate the problem of vanishing gradient. Fig 5.4 shows a sketch map of RNN and LSTM cell, where x stands for input layer, o for output layer and s for the hidden layer. U, V, W is weights and S(t) = f(U*x(t)+W*s(t-1)). We can also see forget gate, input gate and output gate in LSTM that can control the flow of information.

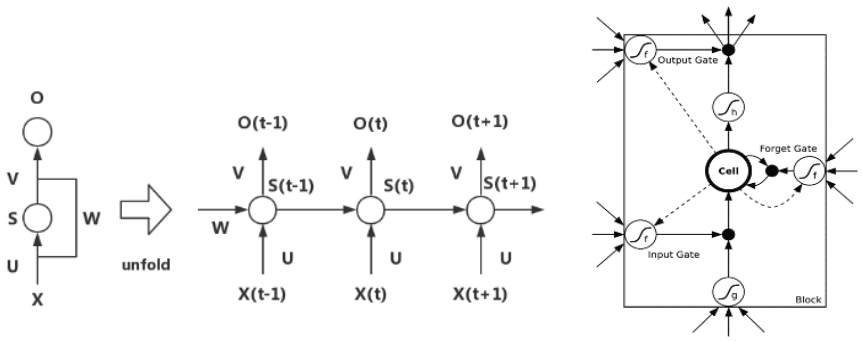

Fig 5.4 The sketch map of RNN (left) and LSTM Cell

In view of the original data of our system is time-series waveform, while the calculation results of each hidden layer in LSTM are related to the current input and the last hidden layer results, we built an LSTM based neural network to classify them. Tensorflow and Keras are used to build our model. The shape of the input array is (3,1024) and the set of the cost function is the same as BPNN.

(3) CNN (Convolutional Neural Networks)

CNNs are a category of Neural Networks that have proven very effective in areas such as classification and image recognition. In image recognition tasks, the nearby pixels typically have a strong relationship with each other, and our data is similar to this situation where the nearby acceleration readings are likely to be correlated in the given data fragments. Thus CNN is chosen as the third model to build in this study. A six-layer CNN was defined for pathological gait classification. The layers are convolution layer 1 whose values are fixed by the input data, pooling layer 1, convolution layer 2, pooling layer 2, the hidden full connection layer and the softmax output layer whose values are derived from previous layers. Wherein, each layer is fully connected to the next layer.

Fig 5.5 demonstrates the structure of CNN in this study. As mentioned before, the shape of input data is (1,3,1024), the shape of convolutional output 1 is (32, 28, 28) with 32

convolutional kernels of size 5 and the shape of max-pooling output 1 is (32, 14, 14) with pooling size of 2 and strides of 2. Similarly, the shape of convolutional output 2 is (64, 14, 14) and the shape of max-pooling output 2 is (64, 7, 7). The dimension of two fully connect layers is 1024 and 6, respectively. The output layer is a softmax classifier.

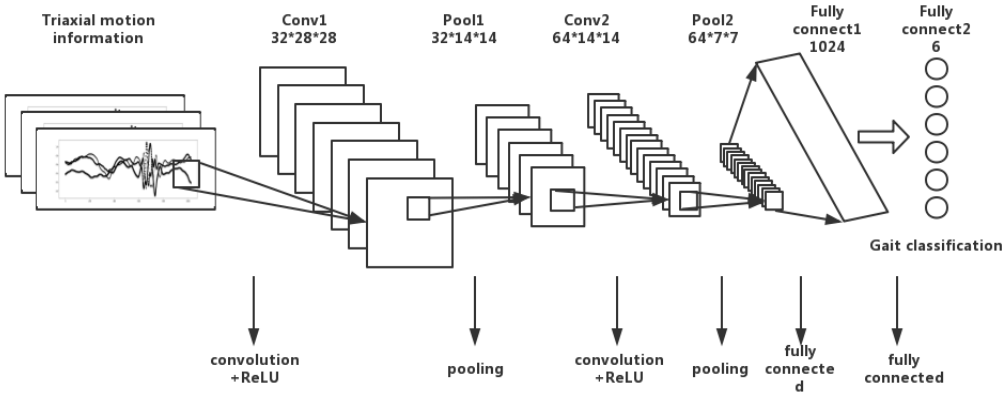

Fig 5.5 The structure of CNN for Pathological Gait Classification

Besides the use of ReLU and softmax like BPNN, the optimization algorithm is set as Adam optimizer that combines the advantages of both the AdaGrad and RMSProp optimization algorithms. The gradient update formula is (5-6):

$$\theta_t = \theta_{t-1} - \alpha * \widehat{m_t}/(\sqrt{\widehat{v_t}} + \varepsilon) \tag{5-6}$$

Where the default learning rate α is set as 0.001, $\varepsilon = 10^{-8}$ just in case the dividend is zero. m_t stands for gradient mean:

$$m_t = \beta_1 m_{t-1} + (1 - \beta_1) g_t \tag{5-7}$$

and v_t stands for gradient variance (5-8):

$$v_t = \beta_2 v_{t-1} + (1 - \beta_2) g_t \tag{5-8}$$

Where β_1, β_2 is exponential attenuation rate, g_t is the gradient at time *t*.

5.2.4 Training Process

The training of all neural networks in this study follows the same process and weight updating rules. To take a general exposition the pseudo-code for our net is proposed.

Algorithm5.1: ANN for pathological gait classification

Input: Labeled train dataset D = $\{((x_i, y_i, z_i),\ L_i\ )\}$,

an unlabeled dataset D(unlabeled) = $\{(x_i, y_i, z_i)\}$

Output: gait type Labels L_{pre} of the unlabeled data

Initialization

random assignment weights and biases of network

Repeat

Forward Propagation:

For each Labeled train data of tri-axises from D:

do

- Calculate the output of the hidden and output layer
- Calculate the deviation between the output layer and the expected output

end

- Use softmax to do classification and update

the weight of each edge in the network

Backward Propagation:

- Conduct backward propagation

Until w_i convergences or training epochs meet n;

Use the trained network to predict the labels

5.3 Results

After preprocessing of the acquired data, we get a labeled motion dataset D $\{((x_i, y_i, z_i),\ L_i\ )\}$ of pathological gait with more than 100 thousand segments. After shuffling, the dataset was split into a training set and test set with a ratio of 0.64. The training set was used to train the model and the test set was used to verify the model when the train finished.

Table 5.1 shows the accuracy of the test for each type of gait and neural network. For BPNN, the hidden layer node was set as 512, the learning rate was 0.003 and batch size, which is the number of training samples in each batch, was set as 200. For LSTM, the learning rate was 0.002 and batch size was set as 128, time steps were set as 5 and neurons in the hidden layer was 128. For CNN, the learning rate was 0.0001 and batch size was set as 128.

Table 5.1 Classification Accuracy of BPNN, LSTM, CNN

Classifier type	**BPNN**	**LSTM**	**CNN**
Hemiplegic gait	96.52%	80.5%	**97%**
Parkinson gait	70.01%	75.8%	**90%**
Natural gait	**93.51%**	83.4%	90%
Gluteus medius gait	**98.56%**	86.2%	93%
Steppage gait	86.42%	83.3%	**93%**
Diplegia gait	75.47%	79.2%	**95%**
Overall Accuracy	86.75%	81.4%	**93%**

From Table I we can observe that for this pathological gait classification task, the precision of CNN are higher than other ANNs, and can reach 93% in four types of gait, which is quite a good performance and proved the great potential of neural

network in pathological gait recognition as well as classification. All neural networks show better in the classification gluteus medius gait and steppage gait, this probably because the two shows a significant difference from other gaits, and meanwhile have more samples in the data set.

Among these three ANNs, BPNN shows more sensitivity to hyperparameters. To evaluate its effect on the accuracy of classification, we train the network with different hidden layer nodes and the results are plotted as Fig 5.6, where f1 value is the harmonic mean of precision (P) and recall (R) rate, that is f1 = 2P*R/(P+R), which is equivalent to the comprehensive evaluation index of accuracy and recall rate. The general trend shows that the accuracy of BPNN rapidly improves from 60 to 256, and shows a peak in 512, then fluctuate smoothly after it. It shows that the specific ration between input nodes and hidden nodes of BPNN was important for the model to learn for further optimizing the network.

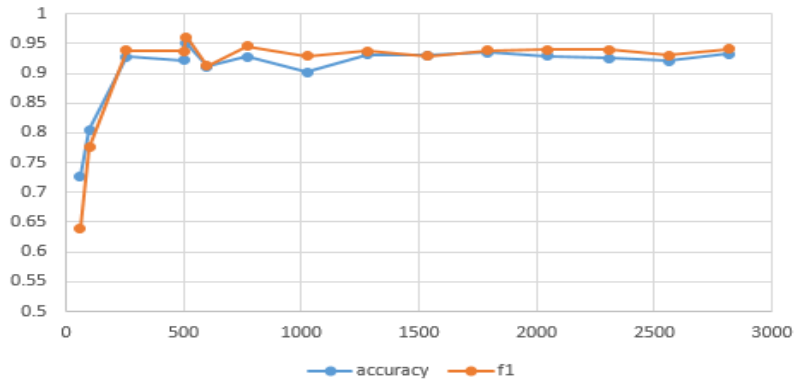

Fig 5.6 The influence of accuracy by hidden nodes in BPNN

It worth to mention that CNN outperforms the other two neural networks on the ability of feature extraction and classification accuracy. A detailed confusion matrix of CNN is shown in Fig 5.7. The confusion matrix is the most basic, intuitive and simplest method to measure the accuracy of the classification model, where the labels

are set as 1 for hemiplegic gait, 2 for Parkinson gait, 3 for natural gait, 4 for gluteus medius gait and 5 for steppage gait.

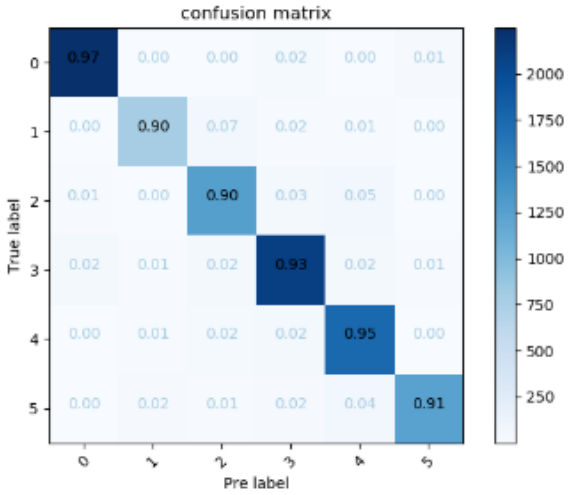

Fig 5.7 The confusion matrix of CNN

In this thesis, an automatic gait identification system based on the motion while using neural networks is proposed. The feasibility of the proposed system is verified on a simulated database and the results are quite promising. However, this is a preliminary study to distinguish normal gait and five pathological gaits. To further validate the robustness of the proposed system, the clinical data will be collected in the future.

5.4 Conclusion

To provide an accurate and affordable measure of pathological gaits identification, an automatic gait recognition system based on the motion signals was proposed in this thesis. The motion signals were fed to three neural networks for classifying the normal gait and five pathological gaits. The proposed system omitted the complex hand-crafted feature extraction process. Experimental results demonstrate the effectiveness of the proposed approach in automatic gait classification. Meanwhile,

the results showed that CNN can achieve better performance in comparison with BPNN and LSTM, which mainly due to the excellent feature extraction capability with the help of convolution kernels. To our best knowledge, this is the first work that involves five pathological modalities and provides the comparison and verification of three neural networks. In the future, larger datasets will be collected in the cooperated hospital to further validate the robustness of the proposed system. Some data fusion technologies like IMU+sEMG based pathological gait classifiers are also worth pursuing.

6 Skeleton Keypoints detection for abnormal gait recognition

Human Keypoint Detection, also known as human posture recognition, aims to locate the position of human joints in the image accurately. As one of the indispensable hot research fields of computer vision, human posture recognition has a large number of landing scenes and broad application prospects. The existing and promising scenarios can be widely used in human gait recognition, rehabilitation training, somatosensory games, augmented reality, etc. Enabled in games, mobile phones, medical care, education, and other fields.

In this part, we exploring unmarked gait information extraction technology of lower limbs for gait analysis. A key point detection system based on the state of the art was used. Clinical data of a patient with abnormal gait was collected in Huashan Hospital, Shanghai. 18 key points of the patient while walking were calculated with a trained neural network. We plot the calculated points in a time domain and then the wave was compared with IMU data. The results show currently deep neural network-based key points detection model is not good enough for abnormal gait recognition. The proposed method omits the complex sensor set-up process and hand-crafted feature extraction process. And, with the ability to act as feature extractors, the proposed method can learn multiple layers of feature hierarchies and realize the classification automatically.

6.1 Methods

6.1.1 Data acquisition experiment setup

In clinical research certain pathological gait are more likely to encounter like hemiplegic gait, parkinsonian gait, etc. For this study, 12 patients with abnormal gait were recruited. Detailed information can be seen in Table 6.1.

Table 6.1 Information of Subjects

No.	gendar	age	Heights(cm)	Weights(kg)
1	Male	44	175	104
2	Male	61	181	80
3	Male	--	165	78
4	Male	24	165	70
5	Male	60	170	58
6	Male	30	180	95
7	Female	18	153	37
8	Male	24	185	60
9	Male	43	176	80
10	Male	42	172	73
11	Female	64	159	55
12	Male	60	165	50
13	Male	48	169	60

The Shimmer 3 IMU and EXG unit are fixed to the outer part of two shins by an elastic bandage, wherein the Y-axis of IMU is set perpendicular to the horizontal plane, the X-axis is perpendicular to the human coronal plane, and the Z-axis is perpendicular to the sagittal plane of the human body. We set the sampling rate of the system to 512Hz and set the IMU's accelerometer sensitivity to ±2g. At the same time, a camera was put behind the subject and keep still. After all set up was done the subjects were asked to walk on standard trails. The triaxial acceleration information of the left and right lower limbs under natural gait is obtained as well as a normal RGB camera-based video. Fig 6.1 shows the placement of Shimmer 3.

Fig 6.1　The placement of Shimmer

Fig 6.2 shows the original triaxial acceleration data, from which we can observe a lower stride frequency and disorderly pace.

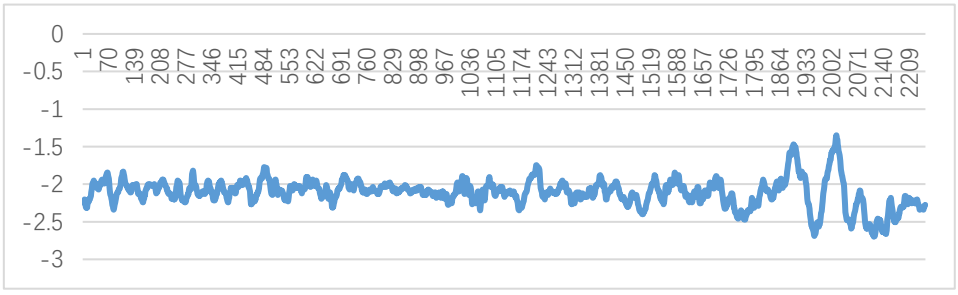

(a)

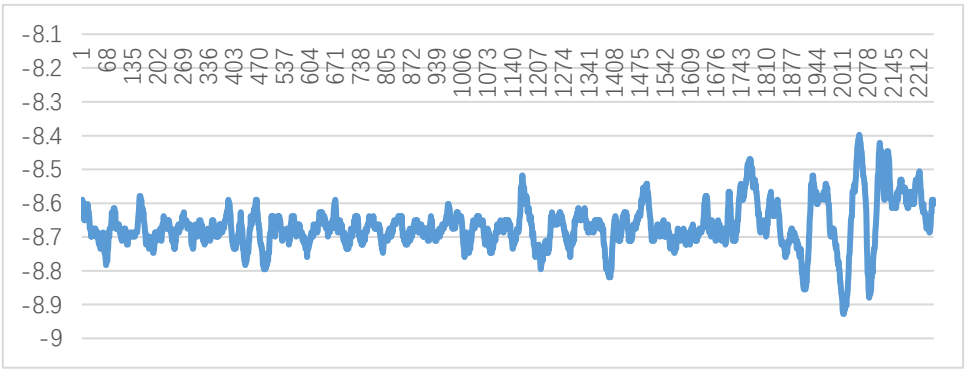

(b)

Fig 6.2　The original triaxial acceleration data (a) x-axis; (b) y-axis

6.1.2 Human Keypoints detection

For human keypoint detection, the champion algorithm of coco2018 was reproduced and used. There are two main ways of human gesture recognition: single-stage and multi-stage. Although the latter is more suitable for the task from rough to fine logic, it seems that the performance is not superior to the single-stage method.

After the emergence of deep convolution network, human pose recognition has developed rapidly. At present, the network structure of the optimal method[46], [47] is relatively simple, mostly using single-stage network design, such as the 2007 COCO Keypoint Challenge Championship method[46] using ResNet-Inception-based network structure, and the latest Simple Baseline[47] using ResNet network structure. Another network structure is a multi-stage network design, that is, a lightweight network as a unified network, and then simply stack it into multi-stage.

They believe that the poor performance of the multi-stage method is mainly due to a variety of unreasonable designs. Their work starts with 1) network design, 2) feature flow and 3) loss function, and proposes a series of improvement measures. The results of their work exceed the existing methods on the MSCOCO Keypoint data set to achieve the best results. The paper has been published in Arxiv. The Overview of Multi-Stage Pose Network(MSPN) can be seen in Fig 6.3.

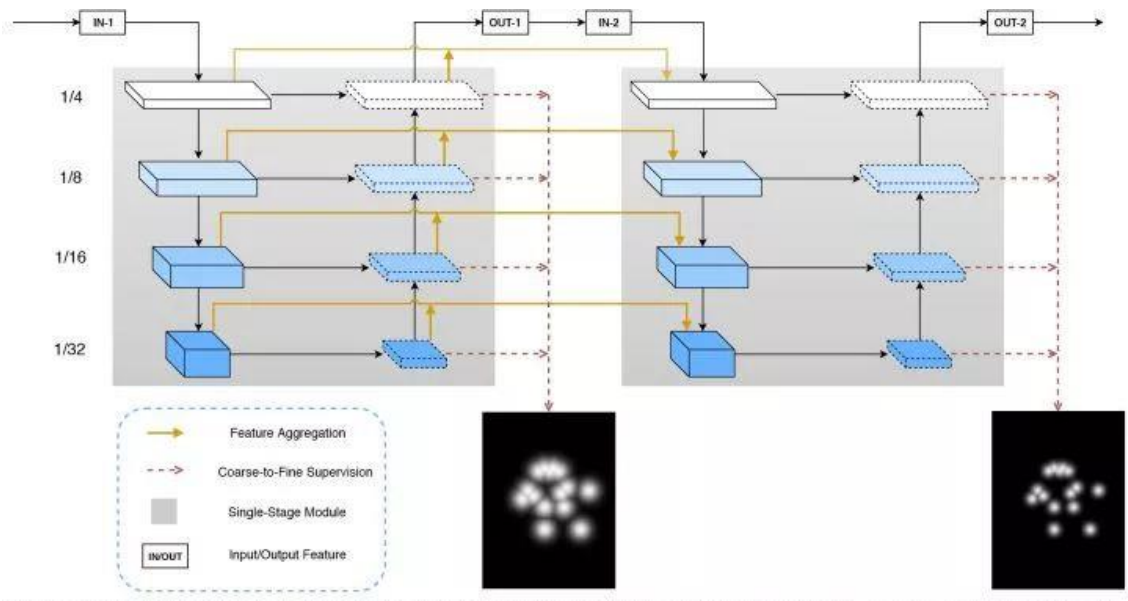

Fig 6.3 Overview of Multi-Stage Pose Network(MSPN)

The multi-stage attitude estimation network MSPN is shown in Figure 6.3. It uses a top-down framework, i.e. the human body detection algorithm is first used to give the human body frame, and then matting, and estimating the pose of a single human body. As mentioned above, there are three new breakthroughs in MSPN: firstly, the network with good image classification performance (such as ResNet) is used as the unit network of multi-stage network; secondly, the information aggregation model is proposed to reduce information loss by stages; thirdly, the coarse-to-fine supervision is introduced and multi-scale supervision is carried out.

6.2 Results

The key points of our clinical video data were recognition by MSPN, the method build before. The results can be seen in fig 6.4 below.

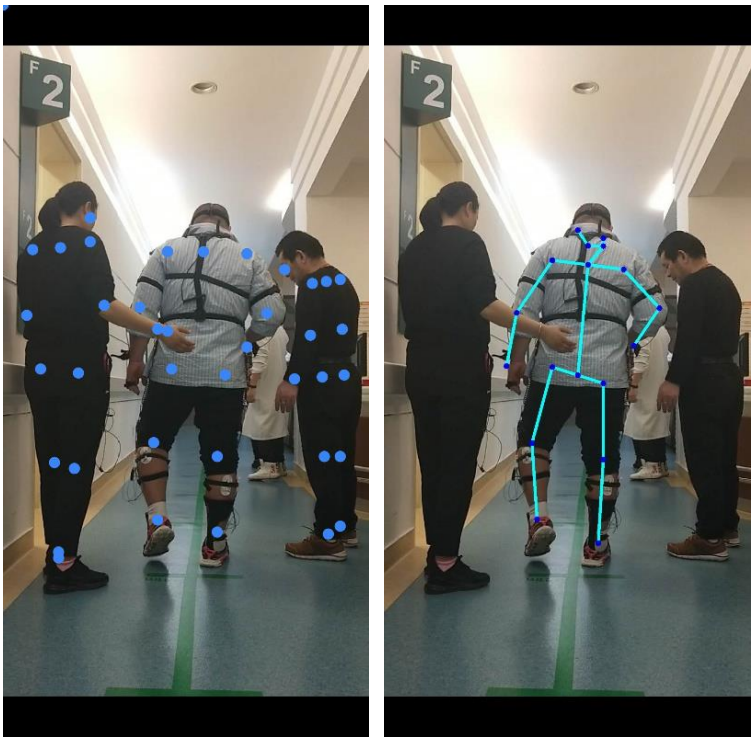

Fig 6.4 Key-points of Skeleton

The raw video is 44Hz, to get time serious points in the space, the original video is converted into a picture set at 20 Hz sampling frequency. And all pictures were detected and a JSON file of 21 key-points of the body in time serious was saved. They are head, left ear, right ear, left eye, right eye, nose, left mouth corner, right mouth corner, neck, left shoulder, right shoulder, left elbow, right elbow, left wrist, right wrist, left hip, right hip, left knee, right knee, left ankle, and right ankle. Each point contains two float number, they are coordinates on the X-Y plane of that point.

Use head as an example, the point's x-coordinate, and they-coordinate location were plotted in the time domain in fig 6.5.

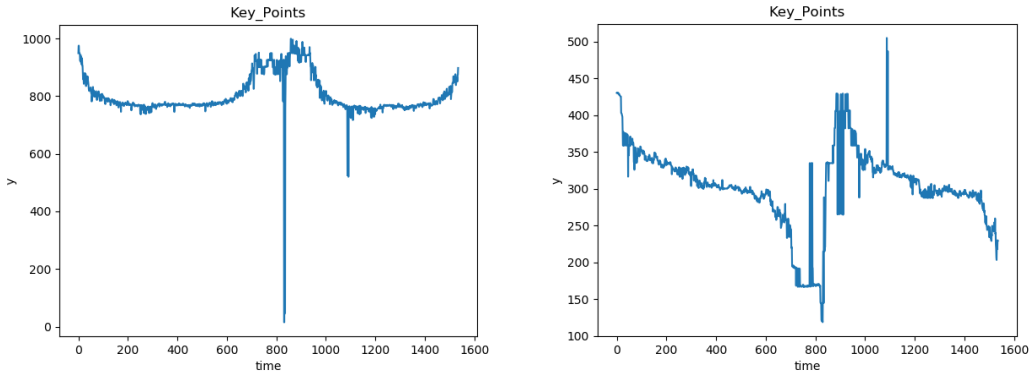

Fig 6.5 The point's x-coordinate(a) and y-coordinate(b) location in time serious

IMU data can be seen in figure 2. Through the analysis and comparison of the data, we can see that when the subjects are within 2 meters of the camera, they can observe the periodic information, but when the subjects leave the camera 2 meters away, the error will increase sharply and lose the periodic information. It is easy to draw a conclusion that the accuracy of the current human keypoint detection technology is not enough to use directly.

6.3 Future works

For future study, a tracking test video acquisition is deserved to be used for a stable point error rate, and the same neural network like the last chapter can be used for the analysis of the gait info from keypoints, thus a video-based abnormal gait classifier system can be released.

Summary

In this thesis, we proposed a lower limb data acquisition system and a neural network-based model for abnormal gait classification. The experiment was designed to collect acceleration signals and sEMG signals under normal and pathological gaits. Data of 15 healthy persons and 15 hemiplegic patients during walking were collected. The classification of gait was carried out based on sEMG and the average accuracy rate can reach 92.8% for CNN. For IMU signals five kinds of abnormal gait are trained based on three models: BPNN, LSTM, and CNN. The experimental results show that the system combined with the neural network can classify different pathological gaits well, and the average accuracy rate of the six-classifications task can reach 93%.

In vision-based research, by using human keypoint detection technology, we obtain the precise location of the key points through the fusion of thermal mapping and offset, thus extracts the space-time information of the key points. However, the results show that even the state-of-the-art is not good enough for replacing IMU in gait analysis and classification. The good news is the rhythm wave can be observed within 2 m, which proves that the temporal and spatial information of the key points extracted is highly correlated with the acceleration information collected by IMU, which paved the way for show visual-based abnormal gait classification algorithm.

Bibliography

[1] R. Caldas, M. Mundt, W. Potthast, F. Buarque de Lima Neto, and B. Markert, "A systematic review of gait analysis methods based on inertial sensors and adaptive algorithms," *Gait Posture*, vol. 57, pp. 204–210, Sep. 2017, doi: 10.1016/j.gaitpost.2017.06.019.

[2] T. N. Nguyen, H. H. Huynh, and J. Meunier, "Skeleton-Based Abnormal Gait Detection," *Sensors*, vol. 16, no. 11, p. 1792, 2016.

[3] M. V. D. Linden, "Gait Analysis, Normal and Pathological Function, 2nd ed. J. Perry, J.M. Burnfield, Slack Inc., 576 pages, ISBN 978-1-55642r-r766-4," *Physiotherapy*, vol. 97, no. 2, pp. 180–180, 2010.

[4] J. P. B. Junior *et al.*, "Applicability of using inertial sensor during gait analysis for hemiplegia patients: Case series," *Gait Posture*, vol. 38, no. 8, pp. S64–S64, 2013.

[5] D. F. Macgregor and R. A. Minns, "GAIT ANALYSIS IN CHILDHOOD HEMIPLEGIA," *Pediatr. Res.*, vol. 32, no. 5, pp. 620–620, 1992.

[6] C. Sun, C. Wang, and W. Lai, "Gait analysis and recognition prediction of the human skeleton based on migration learning," *Phys. Stat. Mech. Its Appl.*, vol. 532, p. 121812, 2019, doi: 10.1016/j.physa.2019.121812.

[7] S. R. Simon, "Quantification of human motion: gait analysis—benefits and limitations to its application to clinical problems," *J. Biomech.*, vol. 37, no. 12, pp. 1869–1880, Dec. 2004, doi: 10.1016/j.jbiomech.2004.02.047.

[8] J. Hannink, T. Kautz, C. Pasluosta, K. G. Gassmann, J. Klucken, and B. Eskofier, "Sensor-based Gait Parameter Extraction with Deep Convolutional Neural Networks," *IEEE J. Biomed. Health Inform.*, vol. 21, no. 1, pp. 85–93, 2016.

[9] W. Tao, T. Liu, R. Zheng, and H. Feng, "Gait Analysis Using Wearable Sensors," *Sensors*, vol. 12, no. 2, pp. 2255–2283, Feb. 2012, doi: 10.3390/s120202255.

[10] H. H. Manap, N. M. Tahir, and R. Abdullah, "Anomalous gait detection using Naive Bayes classifier," in *Industrial Electronics & Applications*, 2012.

[11] T. Chau, "A review of analytical techniques for gait data. Part 1: fuzzy, statistical and fractal methods," *Gait Posture*, vol. 13, no. 1, pp. 49–66, 2001.

[12] T. Chau, "A review of analytical techniques for gait data. Part 2: neural network and wavelet methods," *Gait Posture*, vol. 13, no. 2, pp. 102–120, Apr. 2001, doi: 10.1016/S0966-6362(00)00095-3.

[13] Z. Gandomkar and F. Bahrami, "Proposing a new set of features based on frieze pattern to discriminate normal and abnormal gait," in *Biomedical Engineering*, 2013.

[14] H. Murase and R. Sakai, *Moving object recognition in eigenspace representation: gait analysis and lip reading*. 1996.

[15] E. Desseree-Calais and L. Legrand, "First results of a complete marker-free methodology for human gait analysis," in *IEEE Engineering in Medicine & Biology Conference*, 2005.

[16] S. Jeong, T. Kim, and J. Cho, "Gait recognition using description of shape synthesized by planar homography," *J. Supercomput.*, vol. 65, no. 1, pp. 122–135, 2013.

[17] I. Sarkar, F. Alisherov, T. Kim, and D. Bhattacharyya, "Palm Vein Authentication System: A Review," *Int J Control Autom Syst*, vol. 3, 2010.

[18] H. Ju and B. Bir, “Individual recognition using gait energy image,” *IEEE Trans. Pattern Anal. Mach. Intell.*, vol. 28, no. 2, pp. 316–322, 2005.

[19] P. Theekhanont, W. Kurutach, and S. Miguet, “Gait recognition using GEI and pattern trace transform,” in *International Symposium on Information Technology in Medicine & Education*, 2012.

[20] Howell Adam M., K. Toshiki, Hayes Heather A., F. K Bo, and Bamberg Stacy J. Morris, “Kinetic Gait Analysis Using a Low-Cost Insole,” *IEEE Trans. Biomed. Eng.*, vol. 60, no. 12, pp. 3284–3290, 2013.

[21] C. B. Redd and S. J. M. Bamberg, “A Wireless Sensory Feedback Device for Real-Time Gait Feedback and Training,” *IEEEASME Trans. Mechatron.*, vol. 17, no. 3, pp. 425–433, 2012.

[22] J. Bae, “Gait analysis based on a hidden Markov model,” in *International Conference on Control*, 2012.

[23] M. Yoneyama, Y. Kurihara, K. Watanabe, and H. Mitoma, “Accelerometry-based gait analysis and its application to Parkinson’s disease assessment- part 2: a new measure for quantifying walking behavior,” *IEEE Trans. Neural Syst. Rehabil. Eng.*, vol. 21, no. 6, pp. 999–1005, 2013.

[24] M. Yoneyama, Y. Kurihara, K. Watanabe, and H. Mitoma, “Accelerometry-based gait analysis and its application to Parkinson’s disease assessment–part 1: detection of stride event,” *IEEE Trans Neural Syst Rehabil Eng*, vol. 22, no. 3, pp. 613–622, 2014.

[25] P. C. Chung, Y. L. Hsu, C. Y. Wang, C. W. Lin, J. S. Wang, and M. C. Pai, “Gait analysis for patients with Alzheimer’S disease using a triaxial accelerometer,” in *IEEE International Symposium on Circuits & Systems*, 2012.

[26] C. Senanayake and S. M. N. A. Senanayake, “Human Assisted Tools for Gait Analysis and Intelligent Gait Phase Detection,” in *Innovative Technologies in Intelligent Systems & Industrial Applications, Citisia*, 2009.

[27] Bamberg Stacy J. Morris, Benbasat Ari Y., S. Donna Moxley, Krebs David E., and Paradiso Joseph A., “Gait analysis using a shoe-integrated wireless sensor system,” *IEEE Trans. Inf. Technol. Biomed.*, vol. 12, no. 4, pp. 413–423, 2008.

[28] J. Courtney and A. M. de Paor, “A monocular marker-free gait measurement system,” *IEEE Trans. Neural Syst. Rehabil. Eng. Publ. IEEE Eng. Med. Biol. Soc.*, vol. 18, no. 4, p. 453, 2010.

[29] M. Chen, B. Huang, and Y. Xu, “Human Abnormal Gait Modeling via Hidden Markov Model,” in *International Conference on Information Acquisition*, 2007.

[30] S. Bao, S. Yin, C. Hongyu, and W. Chen, “A wearable multimode system with soft sensors for lower limb activity evaluation and rehabilitation,” 2018, pp. 1–6, doi: 10.1109/I2MTC.2018.8409880.

[31] I. Fentiman, “Clinical Features and Diagnosis,” *Behavior*, vol. 3, no. 2, pp. 41–44, 1991.

[32] D. Tan, K. Huang, S. Yu, and T. Tan, “Efficient Night Gait Recognition Based on Template Matching,” in *International Conference on Pattern Recognition*, 2006.

[33] A. I. Meigal *et al.*, “Novel parameters of surface EMG in patients with Parkinson’s disease and healthy young and old controls,” *J. Electromyogr. Kinesiol. Off. J. Int. Soc. Electrophysiol. Kinesiol.*, vol. 19, no. 3, pp. e206–e213, 2009.

[34] J. Stamatakis, J. Cremers, D. Maquet, B. Macq, and G. Garraux, “Gait feature extraction in Parkinson’s disease using low-cost accelerometers,” in *2011 Annual International Conference of the IEEE Engineering in Medicine and Biology Society*, Boston, MA, 2011, pp. 7900–7903, doi: 10.1109/IEMBS.2011.6091948.

[35] S. Esmaeilzadeh, Y. Yao, and E. Adeli, “End-to-End Parkinson Disease Diagnosis using Brain MR-Images by 3D-CNN,” 2018.

[36] W. Yuan and L. Zhang, “Gait Classification and Identity Authentication Using CNN,” in *Asian Simulation Conference*, 2018.

[37] P. Vieregge, H. Stolze, C. Klein, and I. Heberlein, “Gait quantitation in Parkinson’s disease — locomotor disability and correlation to clinical rating scales,” *J. Neural Transm.*, vol. 104, no. 2–3, pp. 237–248, 1997.

[38] K. M. Iyer, *Clinical Examination in Orthopedics*. 2012.

[39] J. Jankovic, “Gait disorders,” *Neurol. Clin.*, vol. 33, no. 1, pp. 249–268, 2015.

[40] T. A. L. Wren and G. E. G. Iii, “Efficacy of clinical gait analysis: A systematic review,” *Gait Posture*, vol. 34, no. 2, pp. 149–153, 2011.

[41] E. Dolatabadi, B. Taati, and A. Mihailidis, “An Automated Classification of Pathological Gait using Unobtrusive Sensing Technology,” *IEEE Trans. Neural Syst. Rehabil. Eng.*, vol. PP, no. 99, pp. 1–1, 2017.

[42] M. Alaqtash, T. Sarkodie-Gyan, H. Yu, O. Fuentes, R. Brower, and A. Abdelgawad, “Automatic classification of pathological gait patterns using ground reaction forces and machine learning algorithms,” *Conf Proc IEEE Eng Med Biol Soc*, vol. 2011, no. 4, pp. 453–457, 2011.

[43] M. Zeng *et al.*, “Convolutional Neural Networks for Human Activity Recognition using Mobile Sensors,” in *Proceedings of the 6th International Conference on Mobile Computing, Applications and Services*, Austin, United States, 2014, doi: 10.4108/icst.mobicase.2014.257786.

[44] C. K. Du, N. H. Molen, and R. H. Rozendal, “Step length, step frequency and temporal factors of the stride in normal human walking,” *Proc. K. Ned. Akad. Van Wet.*, vol. 73, no. 2, p. 214, 1970.

[45] Y. Lecun, Y. Bengio, and G. Hinton, “Deep learning.,” *Nature*, vol. 521, no. 7553, p. 436, 2015.

[46] Y. Chen, Z. Wang, Y. Peng, Z. Zhang, and S. Jian, “Cascaded Pyramid Network for Multi-Person Pose Estimation,” 2017.

[47] B. Xiao, H. Wu, and Y. Wei, “Simple Baselines for Human Pose Estimation and Tracking,” 2018.

Acknowledgments

The completion of this article is inseparable from the guidance and help I got in the graduate stage. First of all, I want to express my highest appreciation to my supervisor Prof. Wei Chen, she is powerful while easy-going, without her thoughtful guidance and unconditional support I can't achieve these outcomes. The moments in CIME (Center for Intelligent Medical Electronics) will always be shining in the future and become a precious treasure of my life.

I also want to express my sincere thanks to Assoc. Prof. Yu Ma， Assoc. Prof. Dai Chenyu, Dr. Chen Chen from Fudan University and Assoc. Prof Syed Kakakhel from the University of Turku for their help in the thesis writing work. For clinical data collection, thanks to Prof. Junfa Wu from Huashan Hospital, college students Hangyu Zhu, Xinping Wang from Fudan University and all the coordinators in this research.

I also want to thanks all the colleagues in CIME and all the classmates at Fudan University, they build a good memory at Fudan and Turku. Special thanks to my firsts teammate Shenjie Bao, Ph.D. candidate Hongyu Chen, my friend Wei Li, Ya'nan Lu, Haoran Ren and Xiaoyu Wang for their cooperation during my study.

Finally, I would like to thank my parents, grandparents and my lovely girl. Thanks for their support and trust, with them I always feel happy and have more courage to meet the future.

Publications and Awards

Publications

[1] Shenjie Bao, Shubao Yin, Hongyu Chen, Wei Chen. A wearable multimode system with soft sensors for lower limb activity evaluation and rehabilitation[C]//2018 IEEE International Instrumentation and Measurement Technology Conference (I2MTC). IEEE, 2018: 1-6.

[2] Shubao Yin, Chen Chen, Hnagyu Zhu, Xinping Wang, Wei Chen. Neural Network for Pathological Gait Classification Using Wearable Motion Sensor[C]// 2018 IEEE Biomedical Circuits and Systems Conference (BioCAS). IEEE, 2019.

Patents

[1] A wearable signal acquisition system for lower limb rehabilitation and evaluation. Inventors: Shenjie Bao, Wei Chen, Hongyu Chen, Shubao Yin (patent for utility models, application number 201721400281.5, authorized public number: CN 208492094 U)

[2] Plantar pressure signal acquisition system. Inventors: Hongyu Chen, Wei Chen, Shenjie Bao, Shubao Yin (patent for utility models, application number 201721392982.9, authorized public number: CN 208511028 U)

[3] Wearable lower limb rehabilitation and evaluation system. Inventors: Hongyu Chen, Wei Chen, Shenjie Bao, Shubao Yin (patent for invention, application number 201711013940.4)

[4] A gait anomaly classification method based on deep convolution neural network. Inventors: Shubao Yin, Hangyu Zhu, Xinping Wang, Wei Chen. (patent for invention, application number 201910063488.5)

[5] A gait anomaly recognition method based on back propagation neural network. Inventors: Shubao Yin, Hangyu Zhu, Xinping Wang, Wei Chen. (patent for invention, application number 201910064053.2)

[6] Multi-sensor signal fusion method based on deep learning for gait classification. Inventors: Shubao Yin, Hangyu Zhu, Xinping Wang, Wei Chen. (patent for invention, application number 201910063463.5)

Awards

[1] First Prize of 2017 National Undergraduate Biomedical Engineering Innovation Design Competition. Team member: Hongyu Chen, Shenjie Bao, Shubao Yin, mentor: Wei Chen.

[2] First Prize of Medical Service Robot Innovation Design Session in 2018 China Robot Competition. Team member: Shenjie Bao, Hongyu Chen, Shubao Yin, Zeguo Shao, mentor: Wei Chen.

[3] Second Prize of 2017 National college students mathematical modeling contest. Team member: Wei Li, Ya'nan Lu, Shubao Yin, mentor: Wei Chen.